

(AGN)²

14. Active Galactic Nuclei - Results

Week 16
June 17 (Monday), 2024

updated on 06/17 09:25

선광일 (Kwangil Seon)
KASI / UST

14.2 Energy Source

- The luminosity of a typical AGN, of order $10^{12}L_{\odot}$, is far too large for its source to be a star.
 - The most massive stars are of order 10^2M_{\odot} , and have luminosities of 10^5L_{\odot} .
 - Since in such massive stars, the radiation pressure dominates over the gas pressure, and they are close to the limit of instability. More massive stars, producing energy by thermonuclear reaction, cannot exit.
 - Any spherically symmetric object whose gravity holds it together against radiation pressure must satisfy the Eddington condition:

$$L \leq L_{\text{Edd}} = \frac{4\pi c G m_{\text{H}} M}{\sigma_T} = 1.26 \times 10^{38} \frac{M}{M_{\odot}}$$

$$\frac{L}{L_{\odot}} \leq \frac{L_{\text{Edd}}}{L_{\odot}} = 3.22 \times 10^4 \frac{M}{M_{\odot}}$$

Here, σ_T is the electron-scattering, or Thomson cross section, which is the minimum opacity. **Any larger opacity would correspond to a smaller upper limit to the luminosity.**

Based on this, the central source in an AGN with $L = 10^{12}L_{\odot}$ must have $M > 3 \times 10^7 M_{\odot}$.

For more complicated geometries (rather than a spherical symmetric geometry) or if the object is not in a steady state, or if neutral clumps are present, the upper luminosity limit may be surpassed, indicating an even higher mass.

- Furthermore, it must be quite small, because the BLR has a size of order $0.07 \text{ pc} \approx 0.2 \text{ light year}$.
- The continuum variation in many AGNs suggest that the central continuum sources may be even smaller, ranging down to at most one light-weak (optical limit) or even on light-day (X-ray limit).

-
- Accretion Disk [reference] Accretion Power in Astrophysics
3rd Ed., (J. Frank, A. King, D. Raine)
 - Thus, large energies are released in very small volumes in the neighborhood of large masses.
 - Thermonuclear reactions cannot do it. However, **gravitational energy release can**.
 - The most promising physical picture is an accretion disk around a massive black hole.
 - In such a situation, the rest-mass energy of infalling material can be converted into radiation or fast particles with greater efficiency than seems achievable by any other processes we know.
 - The luminosity produce may be written
 - $L = \eta \dot{M}c^2$, where \dot{M} = the accretion rate, and η the efficiency of the process (the fraction of the mass that is converted into energy and does not fall into the black hole.)
 - For instance, $\eta = 10\%$, for an AGN with $L = 10^{12}L_\odot$, the necessary accretion rate is $\dot{M} = 0.7M_\odot \text{ yr}^{-1}$.
 - The Simplest Model
 - a geometrically thin, but optically thick disk.
 - Orbital energy is converted into heat by a viscosity that is related to the gas pressure.
 - Then, the surface temperature of the disk is a function of the accretion rate, black-hole mass, and disk radius. It emits a continuum with spectrum:

$L_\nu = C\nu^{1/3}$ over a limited range of frequency, with a high-energy exponential cutoff corresponding to a Planck function with $T = 10^5$ to 10^6 K.

-
- Relativistic plasma
 - However, the spectrum from the accretion disk is unlike that observed (Figure 13.7) and does not account for the X-ray extension.
 - Radio observations show that relativistic plasma is continuously being generated near the black hole as a consequence of electromagnetic fields connected with rotation.
 - The observations often show narrow jet-like plasma structures extending from close to the source to large distances.
 - They seem likely to be in the axis of rotation of the accretion disk (which is often not the same as the axis of the host galaxy).
 - The generation of the highest-energy photons is intimately connected with the generation and properties of the relativistic plasma.
 - Continuum spectrum
 - Unlike the galactic case, the hydrogen-ionizing continuum can be directly observed from high redshift objects.
 - Figure 14.1 shows such a mean spectrum. The continuum spectrum is fitted by a broken power-law.

$$f_\nu \propto \nu^{-1.76 \pm 0.12} \quad 500\text{\AA} < \lambda < 1200\text{\AA}$$

$$\propto \nu^{-0.69 \pm 0.06} \quad 1200\text{\AA} < \lambda < 3000\text{\AA}$$

- Observationally, there is always a “gap” between $\sim 912\text{\AA}$ and $\gtrsim 0.5\text{ keV}$ ($\lesssim 25\text{\AA}$), the shortest UV wavelength that can be observed and the lowest energy X-rays that can be observed.
- The continuum within this gap is very important in photoionizing clouds.

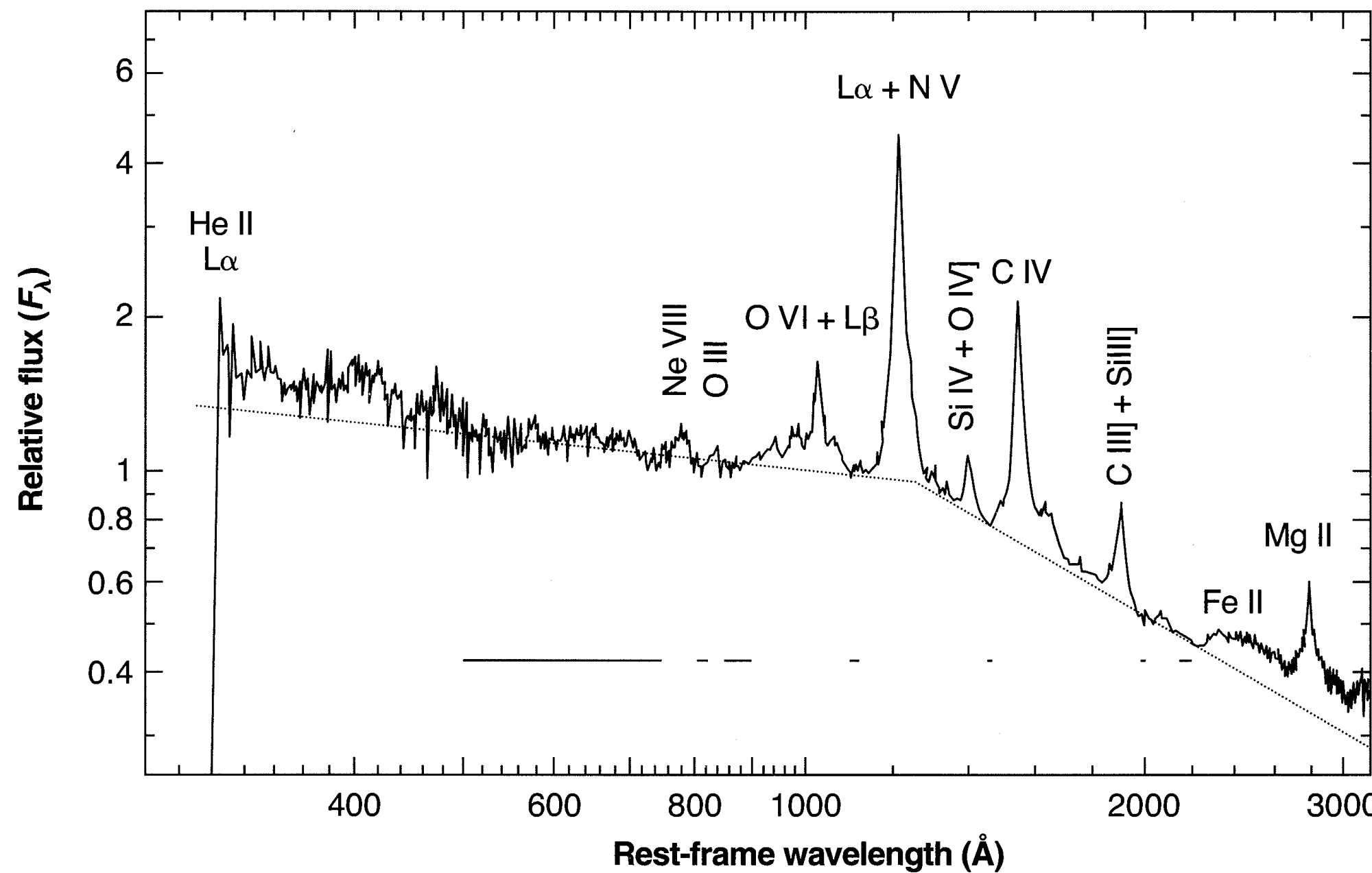


[Figure 14.1]

Overall mean composite spectrum from a sample of intermediate-redshift quasars is shown. The dotted line indicates a fitted broken power-law continuum. (Telfer et al. ApJ, 565, 773). A sample of 332 HST spectra of 184 QSOs with $z > 0.33$ was used.

14.3 Narrow-Line Region

- Modeling
 - The modeling AGNs is exactly the same as that used for PNe and H II regions, but including the additional physical processes relevant for high-energy photons.
 - The structures of the AGNs are far less resolved and there is almost no direct observational information on their forms, shapes, symmetries, degree of fine structure.
 - The simplest method is to assume (1) spherical symmetry for a complete model, or (2) plane-parallel symmetry for a representative dense region (or cloud) far from the central source, and thus illuminated by parallel radiation from it.
 - The actual situation would be far more complicated.

-
- In the best models
 - all the processes described in Chapter 11 were taken into account.
 - Auger transitions in heavy ions
 - Collisional excitation and ionization by the fast electrons produced by the Auger process and by photoionization by high-energy photons.
 - Line excitations by photoionisation leaving the residual ion in an excited level of the ground configuration.
 - Charge-exchange reactions are also important in AGN models.
 - The deduced abundances suggest that refractory elements like Fe are condensed onto grains.
 - Modeling processes:
 - Specify (1) the relative abundances, (2) the electron density, (3) photoionizing spectrum, and (4) the ionization parameter U

$$U = \frac{1}{4\pi r^2 c n_{\text{H}}} \int_{\nu_0}^{\infty} \frac{L_{\nu}}{h\nu} d\nu = \frac{Q(\text{H}^0)}{4\pi r^2 c n_{\text{H}}} \quad \text{defined at the inner face of the cloud.}$$

- Integration is carried forward from the inner face of the cloud into the cloud until the ionization has dropped so low, and the emission lines are negligible.

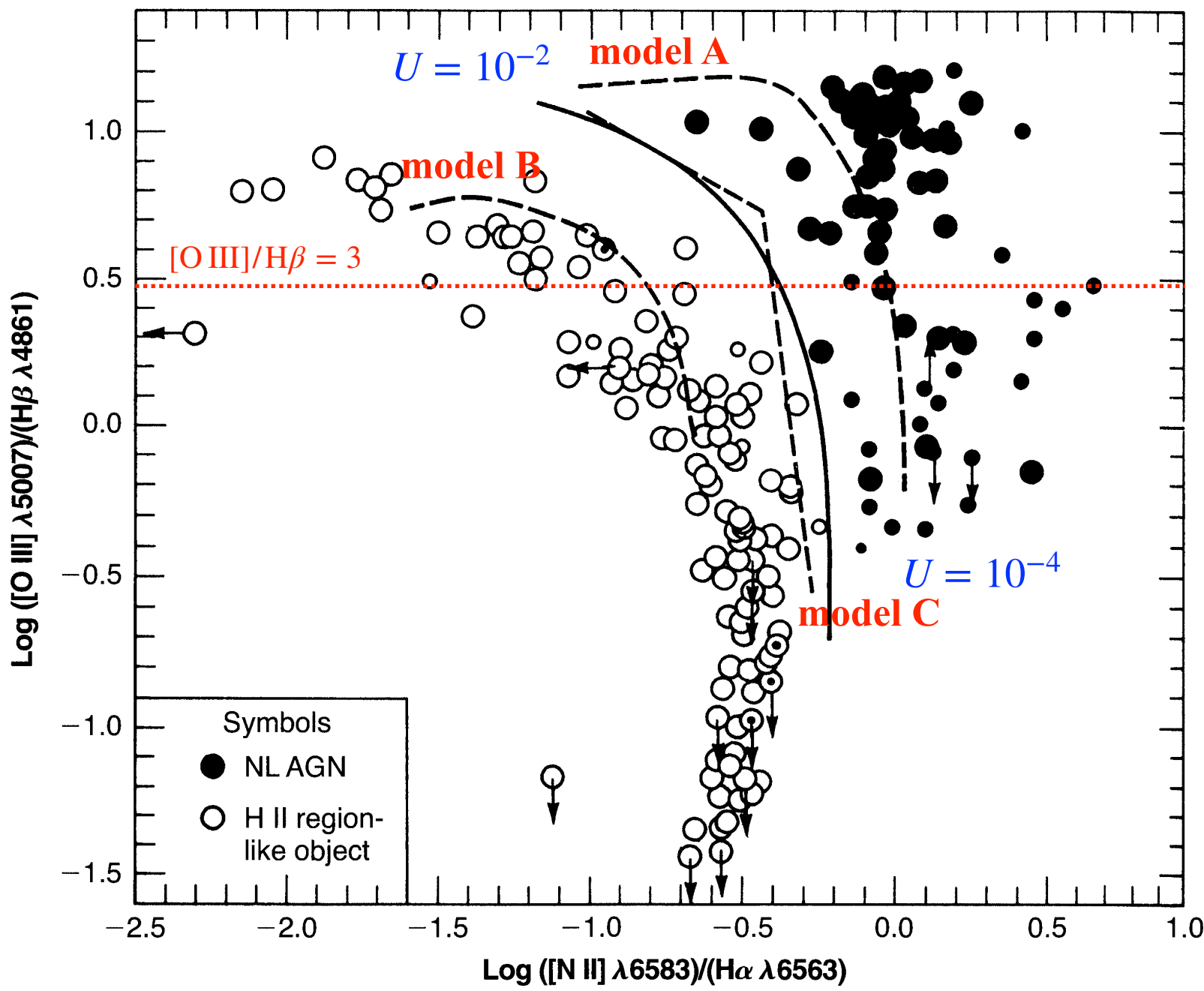
If the physical dimension or optical depth are reasonably known, the integration can be terminated at the specified location.

- Because of collisional-deexcitation effects, the results depend not only upon U but upon n_e as well.
- A more sophisticated model can be built up as a weighted sum of such simple models, with different values of U and n_e , representing a distribution of clouds at different distances r from the central source.

There is thus a great range of possible models.

-
- Comparison of the models with the observational data (Veilleux & Osterbrock 1987)
 - The calculations do not include all of the dust and high-energy effect. (outdated model)
 - The ratios were chosen to give the best separation of the two classes of objects, and to minimize the effects of dust extinction.
 - $[\text{O III}]/\text{H}\beta$ ratio is mainly an indicator of the mean level of ionization and temperature
 - $[\text{OI}]/\text{H}\alpha$ and $[\text{S II}]/\text{H}\alpha$ ratios are indicators of the relative importance of a large partially ionized zone produced by high-energy photoionization.
 - The significance of the $[\text{N II}]/\text{H}\alpha$ ratio is not so immediately obvious.
 - Solid curve on each figure is the best empirical dividing line between the two types of objects.
 - Some of the AGNs close to the dividing line probably contain both OB stars and an active-nucleus hard-photon source.

[Figure 14.2]



Open circles - H II regions in external galaxies, starburst, or HII region galaxies, objects known to be photoionized by OB stars.

Filled circles - AGNs

[model A] - upper dashed curve

- power-law spectrum with $\alpha = 1.5$
- electron density $n_e = 10^3 \text{ cm}^{-3}$
- solar abundance

[model B] - lower dashed curve

- power-law spectrum with $\alpha = 1.5$
- electron density $n_e = 10^3 \text{ cm}^{-3}$
- abundances of heavy elements is reduced by a factor ten.

[model C] - middle dashed curve

- two-component model
- power-law spectrum with $\alpha = 1.5$
- solar abundance
- contains two types of clouds with $n_e = 10^6$ and 10^2 cm^{-3} .
- Both types of clouds have the same ionization parameter.

The ionization parameter varies from $U = 10^{-2}$ at the upper left end of each curve, to $U = 10^{-4}$ at the lower right.

[Figure 14.3]

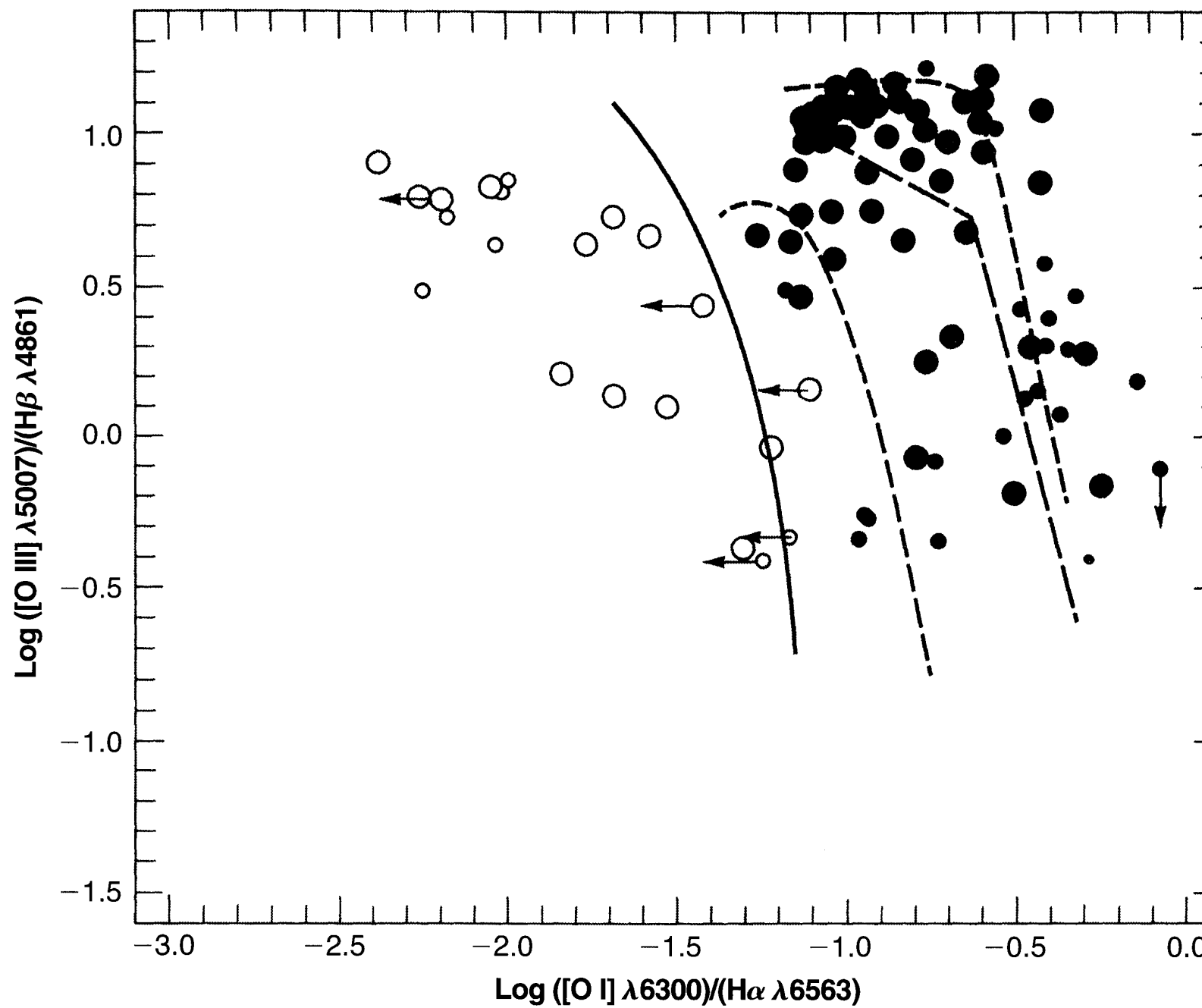
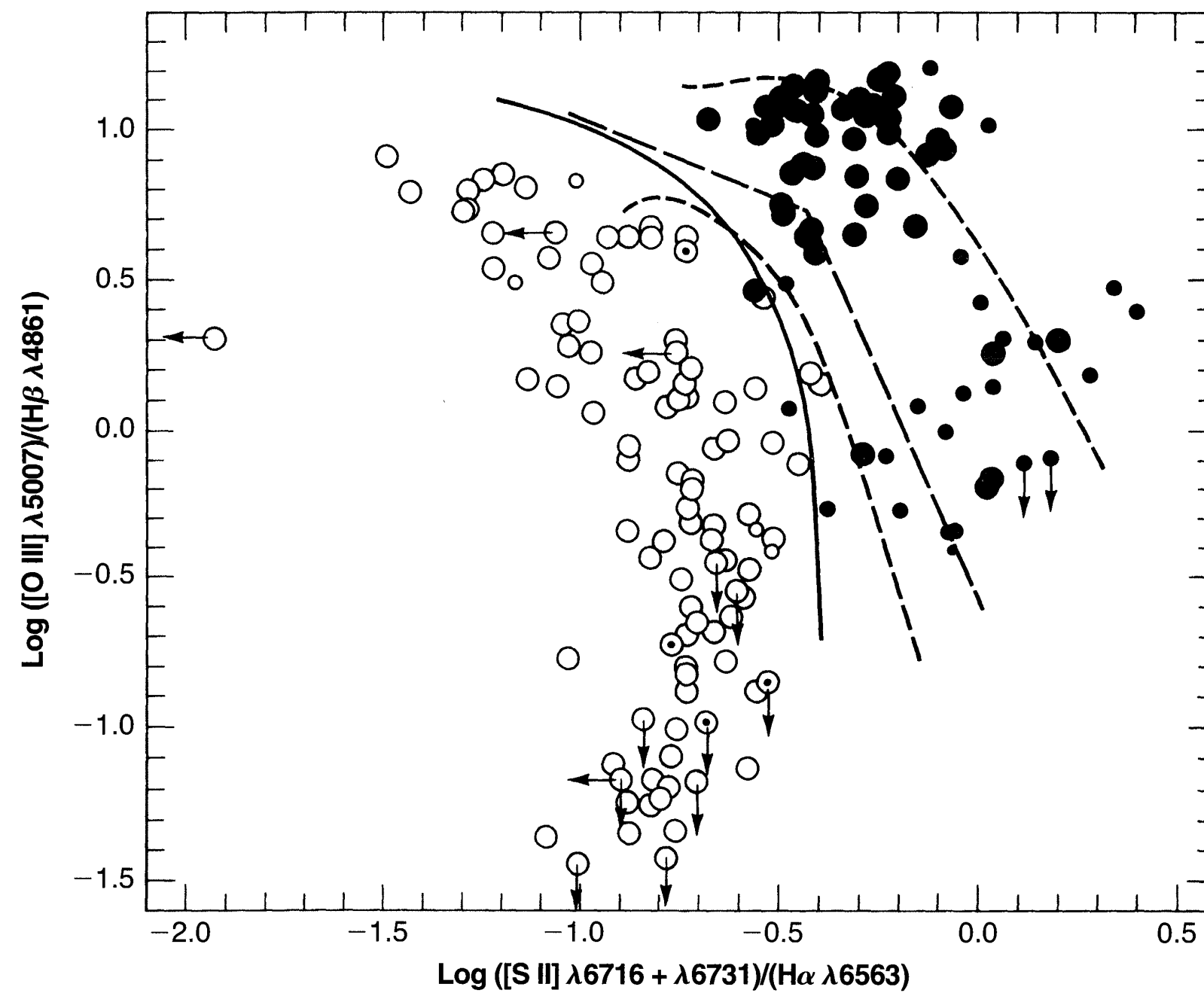


[Figure 14.4]



-
- Simple one-component models
 - The ratios of [S II] and [O I] of AGNs mostly fall between the solar abundance and 0.1 solar abundance simple-model sequences.

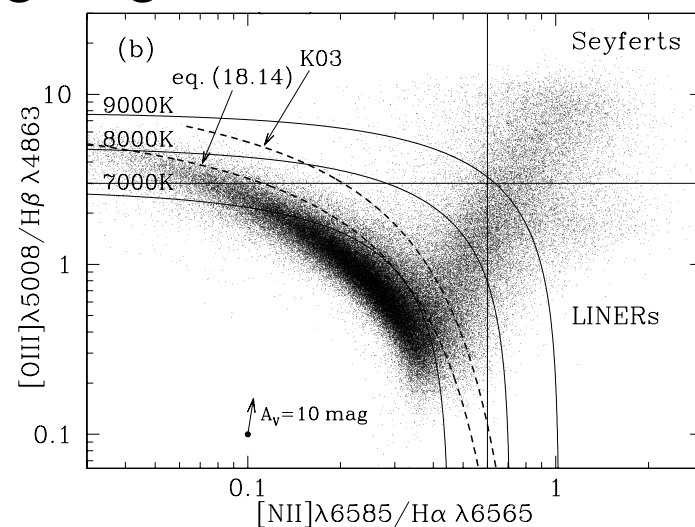
They would roughly agree with abundances averaging about 0.3 of solar abundances with considerable scatter.
 - On the other hand, the [N II] ratio indicate abundances higher than solar; perhaps a factor 1.5 times solar would represent a good average.
 - Since O and H, not N, dominate the cooling, the observed and predicted ratios could be brought into agreement by increasing the N abundance. Thus, N is overabundant with respect to the other heavy elements in these NLRs of typical AGNs.
 - Two-component models
 - The two-component models with solar abundances are displaced from the corresponding simple models (model A) in the direction of lower heavy-element abundances.
 - This is a consequence of collisional deexcitation, which tends to weaken many of the forbidden lines at densities $n_e \approx 10^6 \text{ cm}^{-3}$.
 - Therefore, a higher abundance is required to reproduce the same ratio of an heavy-element line in the simple models (A and B).
 - A wider range of densities would exist in AGNs. Therefore, the simple one-component models tend to underestimate the abundances.

- The two-component models suggest approximately solar abundances of O and S, but a considerable overabundance of N (by a factor of 3).
- However, these abundances are highly model-dependent.
- Other analyses of a few specific AGNs, based on more sophisticated models, have given essentially solar abundances for all three elements.
- The two-component models do not predict $[\text{Fe VII}] \lambda 6087$ and $[\text{Fe X}] \lambda 6375$ as strong as observed in many Seyfert 2 nuclei.
 - However, Models with a continuous distribution of gas, extending in close to the ionizing source do in fact predict [Fe VII] and [Fe X] with roughly the observed intensities.

14.4 LINERs

- Low-Ionization Nuclear Emission-line Regions
 - Seyfert 2 galaxies have relatively high ionization. All the classical objects of this type have $[\text{O III}] \lambda 5007/\text{H}\beta > 3$, and for most of them it is > 5 .
 - Most starburst and H II region galaxies have $[\text{O III}] \lambda 5007/\text{H}\beta < 3$. But, not all galactic nuclei that have $[\text{O III}] \lambda 5007/\text{H}\beta < 3$ are photoionized by OB stars.
 - An appreciable fraction of these low-ionization galaxies have stronger $[\text{O I}] \lambda 6300$ and $[\text{S II}] \lambda\lambda 6716, 6731$ than in H II regions or starburst galaxies
 - First identified by T. M. Heckman (1980)
- Observational Definition of LINERs
 - The original observational definition of a LINER was a galaxy nucleus with emission-line ratios $[\text{O II}] \lambda 3727/[\text{O III}] \lambda 5007 > 1$ and $[\text{O I}] \lambda 6300/[\text{O III}] \lambda 5700 > 1/3$.
 - The first of these criteria is satisfied by many H II region galaxies, but the second is not.
 - A better definition is

$[\text{O III}] \lambda 5007/\text{H}\beta < 3$
 $[\text{O I}] \lambda 6300/\text{H}\alpha < 0.05$
 $[\text{S II}] \lambda 6716 + \lambda 6731/\text{H}\alpha > 0.4$
 $[\text{N II}] \lambda 6583/\text{H}\alpha > 0.5$
 - This definition is adopted because of the difficulties of making comparisons with $[\text{O II}] \lambda 3727$, which can be strongly affected by interstellar extinction.



SDSS, B. Draine

- Stellar Absorption-Lines
 - In many LINERs and H II region galaxies, the emission lines are quite faint, and badly affected by the underlying integrated absorption-line spectrum of the stars in and near the nucleus.
 - This is especially true at $H\beta$ and $H\alpha$, which are seen as absorption lines in almost all galaxies; their strengths depends on the spectral type.
 - It is therefore necessary to correct the observed spectrum for the underlying galaxy spectrum. This can be done by subtracting a template spectrum of a galaxy without emission lines.

All galaxies do not have identical absorption-line spectra, so the real problem is to subtract the spectrum of the galaxy that have the same population of stars and no ionized gas.

This is impossible to fulfill exactly, is impossible even in principle, since the stellar population, the amount of gas, the elemental abundances in it, and the ionization conditions are all linked through the past evolutionary history of the galaxy.
 - The best approximations are (1) to take the spectrum of another galaxy with very weak emission lines, or (2) to add the spectra of representative stars of various spectral types to form a weighted average absorption-line spectrum template.
 - [TEST] It should cancels out the absorption lines that are not at the positions of the emission lines, leaving only the latter and an essentially featureless continuum or nearly zero flux.
- Fractions
 - Among S0, Sa and Sab galaxies, ~53% are LINERs.
 - Among Sb-Sbc galaxies, ~34% are LINERs.
 - 46% of the nuclei of ellipticals show LINER spectra.
 - LINERs also may be commonly found in luminous infrared galaxies (LIRGs).

- Nature of LINERs
 - Initially, it was suggested that they might be examples of objects in which shock-wave heating rather than photoionization is the main energy input mechanism.
 - However, it now seems certain that LINERs are simply the extension, to lower luminosities, smaller ionization parameters, and somewhat larger exponents α in the representative power-law spectrum of Seyfert 2 nuclei.
 - There is no evidence at all favoring shock-wave heating in LINERs.
- LINERs in elliptical galaxies
 - Elliptical galaxies have much weaker emission lines than in spirals.
 - But, 46% of the nuclei of ellipticals do have LINER spectra.
 - The two best known, bright examples with the strongest emission-line spectra are NGC 1052 and NGC 4278.

However, even in them, the emission lines are not strong and are badly blended with the absorption lines of the integrated stellar continuum.
 - In NGC 1052
 - ▶ [O II] $\lambda\lambda 3726, 3729$ lines are partially resolved.
 - ▶ They and [S II] $\lambda\lambda 6716, 6731$ give an electron density $n_e \approx 2 - 3 \times 10^2 \text{ cm}^{-3}$.
 - ▶ A mass of ionized gas $M_{\text{ion}} > 5 \times 10^5 M_\odot$ from the observed H α luminosity
 - The source of ionization in these elliptical galaxy LINERs is photoionization, just as in the spirals.

14.5 Broad-Line Region

- Understanding the BLRs
 - Broad permitted emission lines are the characteristic feature of Seyfert 1 galaxies, BLRG nuclei, quasars, and QSOs.
 - They arise in the small, dense regions close to the central ionizing source.
 - Because the density within them is so high ($n_e \approx 10^9 \text{ cm}^{-3}$ or even higher), the physics is far more complicated than in the narrow-line regions, or in PNe, and H II regions.
 - In many aspects, the BLRs are physically as closely related to stellar atmospheres.
 - Thus, the conclusions that can be drawn from the observations are more highly model-dependent than for nebulae, and hence less certain.
- A simple model: Consider a dense cloud close to the photoionizing source.
 - If the electron density is $n_e = 10^{10} \text{ cm}^{-3}$ and the cloudy is located at 0.1 pc from the source, the ionization parameter U is the same as for a typical NLR with $n_e = 10^5 \text{ cm}^{-3}$ at $d = 30 \text{ pc}$.
 - Figure 14.5 and Table 14.1 show a photoionization model of the thermal and ionization structure of a cloud, with solar abundances, irradiated by a power-law continuum of $f_\nu \propto \nu^{-1.5}$ and an ionization parameter of $U = 10^{-1.5}$.
 - Density: The density is so high that the forbidden lines are all greatly weakened by collisional deexcitation.
 - Temperature: The temperature is raised to the point at which the energy is radiated away by collisionally excited permitted and intercombination lines (mostly in the UV, C IV $\lambda 1549$, C III] $\lambda 1909$, and also H I Ly α).

The calculated temperatures in the BLR models are somewhat higher than in NLR models, because of the increased collisional deexcitation. But, $T \approx 15,000 \text{ K}$ is perhaps a typical value, since the radiative cooling rises steeply with temperature.

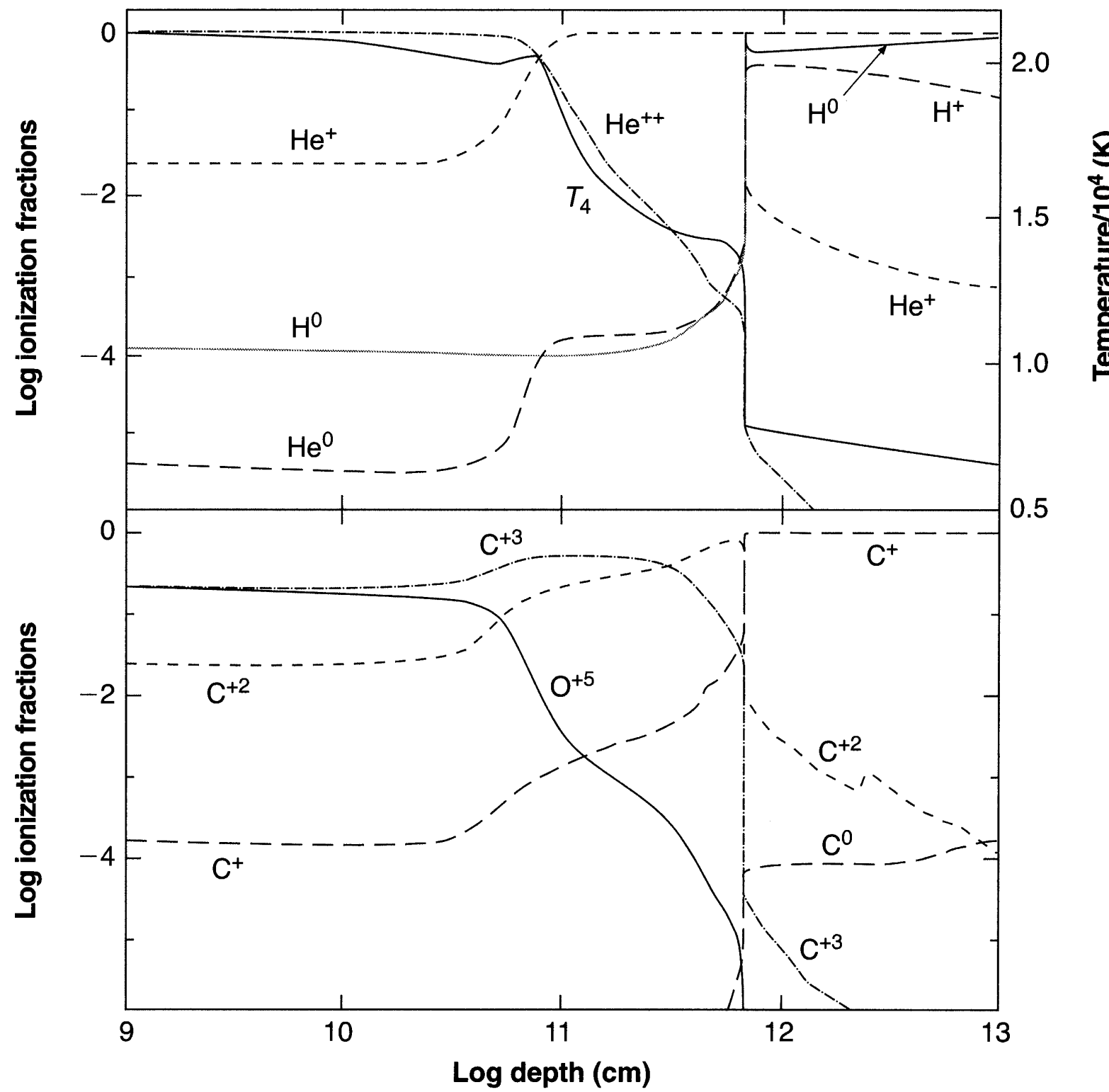


[Figure 14.5]
The ionization structure of a model BLR cloud.

Density $n_e = 10^{-1.5}$
Ionization parameter $U = 10^{10} \text{ cm}^{-3}$
 $\alpha = -1.5$ power-law ionizing continuum.

The calculation stopped at a column density of 10^{23} cm^{-2} .

A region of warm and partially ionized gas extends beyond the hydrogen ionization front due to photoionization of $n = 2 \text{ H}^0$ and penetration of X-rays.

Table 14.1
Observed and predicted relative BLR emission-line intensities

Ion	λ (Å)	Observed ^a	$U = 10^{-1.5}$ Model	Multi-component Model
O VI	1034	0.1–0.3	0.019	0.16
L α	1216	1.00	1.00	1.00
N V	1240	0.1–0.3	0.039	0.04
Si IV + O IV	~1400	0.08–0.24	0.091	0.06
C IV	1549	0.4–0.6	0.77	0.57
He II + O III]	1666	0.09–0.2	0.13	0.14
C III] + Si III]	1909	0.15–0.3	0.077	0.12
Mg II	2798	0.15–0.3	0.16	0.34
H β	4861	0.07–0.2	0.045	0.09

a. The observed intensities from a sample of intermediate ($z \approx 2$) redshift quasars.

-
- Optical-depth and radiative-transfer effects are very important in the BLRs.
 - $\tau_0 \approx 10^2$ at the Lyman limit, since much of the ionization occurs by high-energy photons.
 $\tau_{0l} \approx 10^6$ at the Ly α line center. (only for thermal Doppler broadening. the velocity field would vary significantly over large distances, then it is an overestimation.)
 - Hence, a Ly α line photon emitted in the cloud is scattered many times before it escapes or is absorbed in some other process.
 - Escape probability formalism
 - ▶ The full physical problem, taking into account the variation of emission and absorption with depth into the ionized cloud, and with frequency in the line profile, is a complicated one.
 - ▶ The simplest way to handle the problem is by the escape probability formalism.
 - ▶ Mean number of scatterings a typical resonance-line photon suffers before it escapes depends on geometry, the velocity field, and the line redistribution function, but are approximately given by
- $n_{\text{esc}} \approx 1 + \tau_{0l}$: the number of scatterings a line photon undergoes before escaping
(see [Seon & Kim, 2020, ApJS, 250, 9](#))
- $$\epsilon_{\text{esc}} = \frac{1}{n_{\text{esc}}} \approx \frac{1}{1 + \tau_{0l}}$$
- : the escape probability
- ▶ Therefore, a Ly α photon is scattered roughly 10^6 times before escaping, in a cloud with $\tau_{0l}(\text{Ly}\alpha) = 10^6$. In other words, the escape probability, the probability of escape in a single scattering is $1/n_{\text{esc}} = 10^{-6}$ for $\tau_{0l}(\text{Ly}\alpha) = 10^6$.

- Radiative Transfer Effect of Ly α
 - In an optically thin nebula, every time an H 0 atom reaches $2\ ^2P^o$ (as a result of recombination, cascading down from higher levels, or collisional excitation from the ground level), it spends a mean lifetime $\tau_{2\ ^2P} = 1/A_{2\ ^2P, 1\ ^2S} = 1.6 \times 10^{-9}$ s in the excited level before decaying.
 - But, in an optically thick nebula, the photon emitted does not escape directly, but instead is absorbed, which leads to another radiative excitation to $2\ ^2P^o$, so it is emitted again, and so on. Thus, the average time that some atom spends in this excited level is increased to $n_{\text{esc}}\tau_{2\ ^2P} \approx 1.6 \times 10^{-3}$ s. This is a very large increase.
 - ▶ Hence, the population in the $2\ ^2P^o$ level is quite significant.
 - ▶ Consequently, photoionization from $2\ ^2S$ and $2\ ^2P^o$ levels is important.
 - ▶ This creates a warm and partially ionized region extending beyond the hydrogen ionization front, as shown in Figure 14.5.
- Radiative transfer Effect of H α
 - Since the electron density in the BLR region is high, collisional excitation to other levels $n\ ^2L$ can occur, leading to collisional contributions to the excited Balmer, Paschen, etc., lines.
 - Since transitions to the $3\ ^2L$ levels have the smallest threshold and largest cross sections, H α is especially favored over collisions to higher levels.
 - Angular momentum-changing collisional transitions between $2\ ^2P^o$ and $2\ ^2S$ have zero threshold energy and are even more favored, coupling their populations.
 - ▶ The finite populations in these two levels make for non-negligible optical depths in the Balmer lines, and hence lead to radiative-transfer effects on them.

-
- Ly α photon destroy
 - A Ly α photon (with energy $(3/4)h\nu_0 = 10.2 \text{ eV}$) is an ionizing photon for H 0 atoms in the excited 2 2S and 2 $^2P^o$ levels (threshold energy $(1/4)h\nu_0 = 3.4 \text{ eV}$).

Since they have significant populations, this process occurs, “destroying” at least the Ly α photon absorbed, and often also the one that originally leads to the population of the 2 $^2P^o$ level that absorbed it.

- Ly α photons can be destroyed by collisional deexcitation of 2 $^2P^o$.

If the Ly α photon escaped freely, the critical density for this process would be

$$n_c(2^2P) = \frac{A_{2^2P, 1^2S}}{q_{2^2P, 1^2S}} = 8.7 \times 10^{16} \text{ cm}^{-3} \text{ at } T = 10,000 \text{ K.}$$

- But, in the optically thick case, the mean lifetime in the excited state is increased by a factor n_{esc} , corresponding to decreasing the effective transition probability, and hence the critical density, by the same factor. For the example with $\tau_{0l} = 10^6$

$$n_c(2^2P) = \frac{A_{2^2P, 1^2S}}{n_{\text{esc}} q_{2^2P, 1^2S}} = 8.7 \times 10^{10} \text{ cm}^{-3} \text{ for } \tau_{0l} = 10^6.$$

- This density is relatively high in comparison with the mean density $n_e = 10^9 \text{ cm}^{-3}$ derived for a typical BLR, but may well be reached in some parts of some BLRs.

-
- A homogeneous pure H slab “models” (Table 14.2)
 - All these processes must be taken into account in calculating the BL H I spectrum.
 - Parameters:
 - ▶ constant electron density $n_e = 10^{10} \text{ cm}^{-3}$ and optical depth $\tau_{0l}(\text{Ly}\alpha) = 5 \times 10^6$
 - ▶ Constant temperature is assumed over the cloud.
 - ▶ Increasing the ionization parameter U corresponds to increasing the flux of ionizing photons entered the cloud.
 - The optical depth in $\text{H}\alpha$, $\tau_{0l}(\text{H}\alpha)$, increases since the number of $\text{Ly}\alpha$ photons produced per unit area is also increases.
 - Constant temperature models are quite unrealistic, but illustrates some of the effects involved.

Table 14.2
Relative emission-line intensities in homogeneous BLR models

U	10^{-6}	10^{-4}	10^{-2}	10^0
T (K)	8,000	10,000	14,000	16,000
$\text{H}\beta$ (Case B)	0.82	0.77	4.52	36.23
$\text{H}\alpha$	4.85	4.94	5.70	4.17
$\text{H}\beta$	1.00	1.00	1.00	1.00
$\text{H}\gamma$	0.472	0.265	0.324	0.319
$\text{L}\alpha$	250.0	20.3	30.5	96.0
$2h\nu$	0.602	0.126	0.131	0.130
$\tau_{0l}(\text{H}\alpha)$	1.34	1.11×10^3	5.48×10^3	4.18×10^4

-
- At low T and U , most of the H is neutral, collisional excitation is significant, and therefore $\text{H}\alpha/\text{H}\beta$ and $\text{Ly}\alpha/\text{Ly}\beta$ are larger than their recombination values.

At the lowest U , $\text{H}\beta$ has a slight collisional enhancement relative to Case B.

As U and $\tau_{0l}(\text{H}\alpha)$ increases, the hydrogen lines become fainter relative to Case B due to line self-absorption.

- The competition between collisions and recombination, as well as the radiative-transfer effects in the Balmer lines, make the $\text{Ly}\alpha/\text{Ly}\beta$ ratio first decrease, then increase, along the sequence as listed.
- $\text{Ly}\alpha/\text{H}\beta$ ratio is a straightforward indication of deviations from a pure recombination H I spectrum.
 - Under Case B conditions, in the low-density limit, approximately 2/3 of all recombinations go through 2^2P and lead to $\text{Ly}\alpha$ emission (0.677 at $T = 10^4$ K), while the remainder go through 2^2S and emit the two-photon continuum. The ratio of recombination-line intensities is

$$\frac{j_{\text{Ly}\alpha}}{j_{\text{H}\beta}} = 0.677 \frac{\alpha_B}{\alpha_{\text{H}\beta}^{\text{eff}}} \frac{h\nu_{\text{Ly}\alpha}}{h\nu_{\text{H}\alpha}} = 23.1$$

- In the high-density limit, collisions transfer atoms in the 2^2S level to 2^2P^o before they emit the two-photon continuum, and the intensity ratio is

$$\frac{j_{\text{Ly}\alpha}}{j_{\text{H}\beta}} = \frac{\alpha_B}{\alpha_{\text{H}\beta}^{\text{eff}}} \frac{h\nu_{\text{Ly}\alpha}}{h\nu_{\text{H}\alpha}} = 34.2$$

- Observations indicate that the pure recombination conditions do not apply in BLRs of $z \approx 2$ quasars.
 $\text{Ly}\alpha/\text{H}\beta \approx 10$ rather than ~ 23 or 34 .
- How much of the discrepancy is due to the high-density effects or due to extinction by dust is still not clear.

- Table 14.1
 - The simple model in Figure 14.5 is compared with the observed intensities of the stronger lines for a sample of $z \approx 2$ quasars.
 - ▶ Many lines lie within a factor of two of the observed values.
 - ▶ The model is clearly an oversimplification. BLR gas exists over a broad range of distances from the central object. There is likely to be a broad range of densities as well.
 - The result from a model of the inner regions of AGNs that treats the clouds using distribution functions in radius and density is also shown in the last column.
 - ▶ The overall match is better, with the major exception of N V $\lambda 1240$. This may indicate an overabundance of N in the BLR, similar to that for NLR.

[Table 14.1]
Observed and predicted relative
BLR emission-line intensities

The observed intensities are from a
sample of $z \approx 2$ quasars.

Ion	λ (Å)	Observed ^a	$U = 10^{-1.5}$ Model	Multi-component Model
O VI	1034	0.1–0.3	0.019	0.16
L α	1216	1.00	1.00	1.00
N V	1240	0.1–0.3	0.039	0.04
Si IV + O IV	~1400	0.08–0.24	0.091	0.06
C IV	1549	0.4–0.6	0.77	0.57
He II + O III]	1666	0.09–0.2	0.13	0.14
C III] + Si III]	1909	0.15–0.3	0.077	0.12
Mg II	2798	0.15–0.3	0.16	0.34
H β	4861	0.07–0.2	0.045	0.09

- Permitted broad Fe II lines
 - They are observed in both the optical and UV spectra of many Seyfert 1s and QSOs.
 - In Figure 14.6, the strongest optical Fe II features marked $\lambda\lambda 4570, 5190$, and 5320 are unresolved blends of lines of several multiplets.

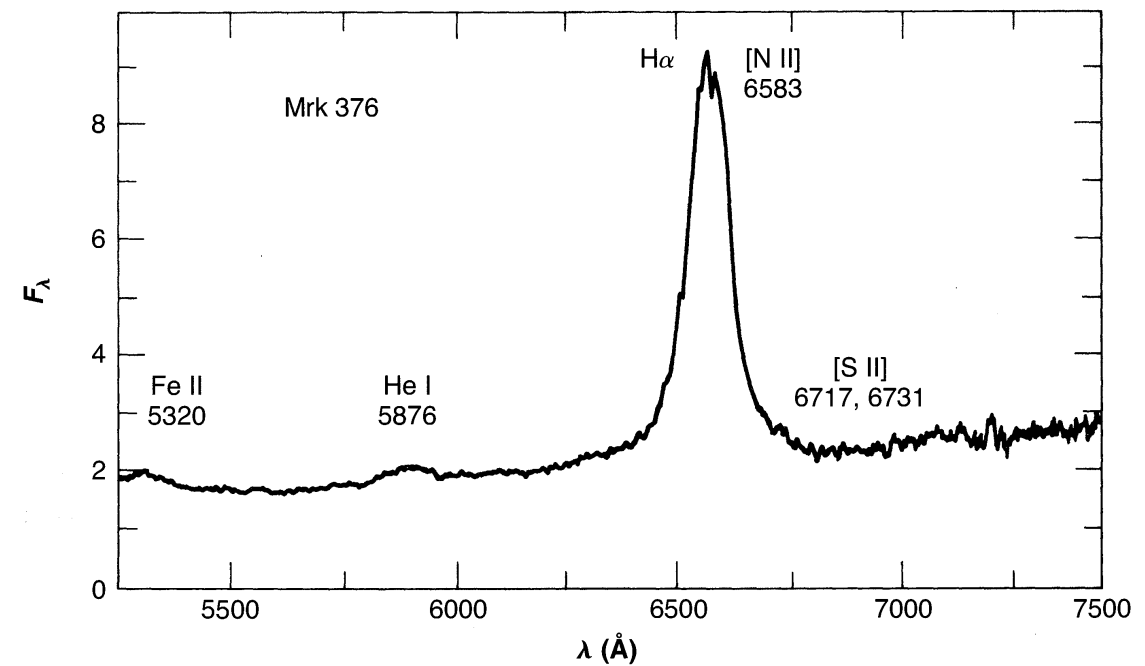
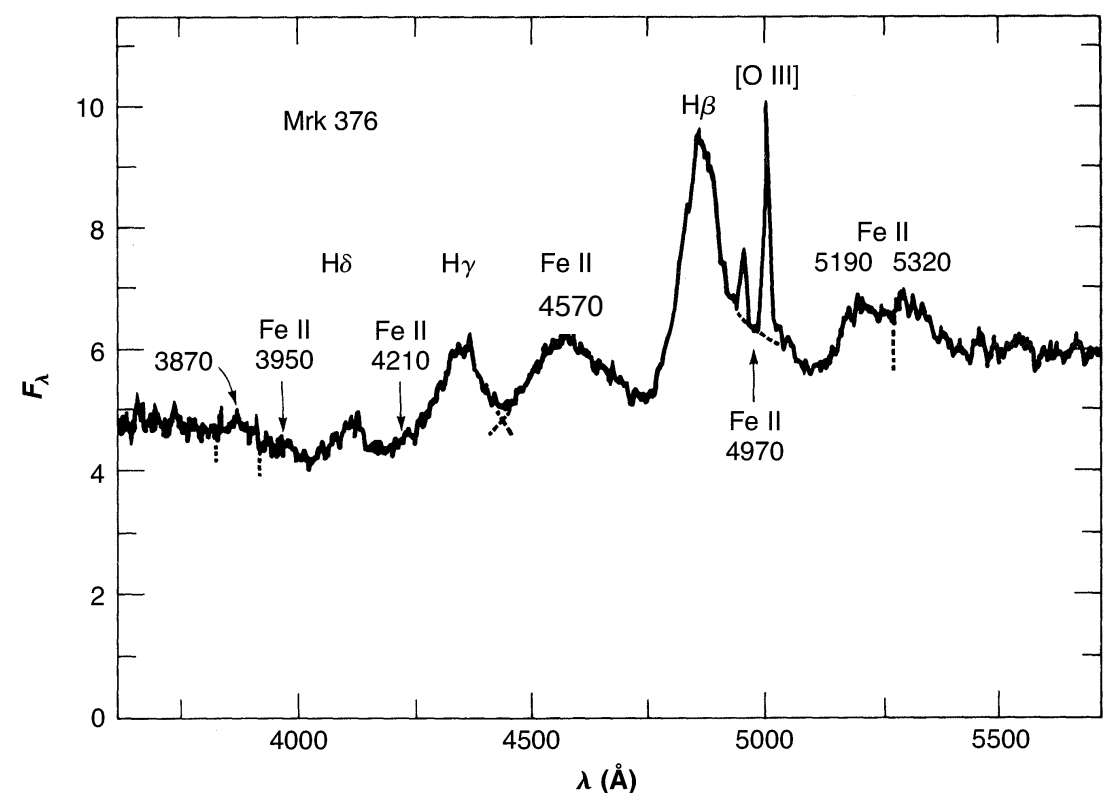


[Figure 14.6]
Spectra of Mrk 376 (Seyfert 1) with strong, broad Fe II and H I emission lines.

- Figure 14.7 shows significantly narrower line widths.

The wavelengths of the individual Fe II lines, grouped by multiplets, are shown in the bottom panel (the spectrum of I Zw 1).

Note that the few individually resolved Fe II lines have essentially the same line widths as H β .

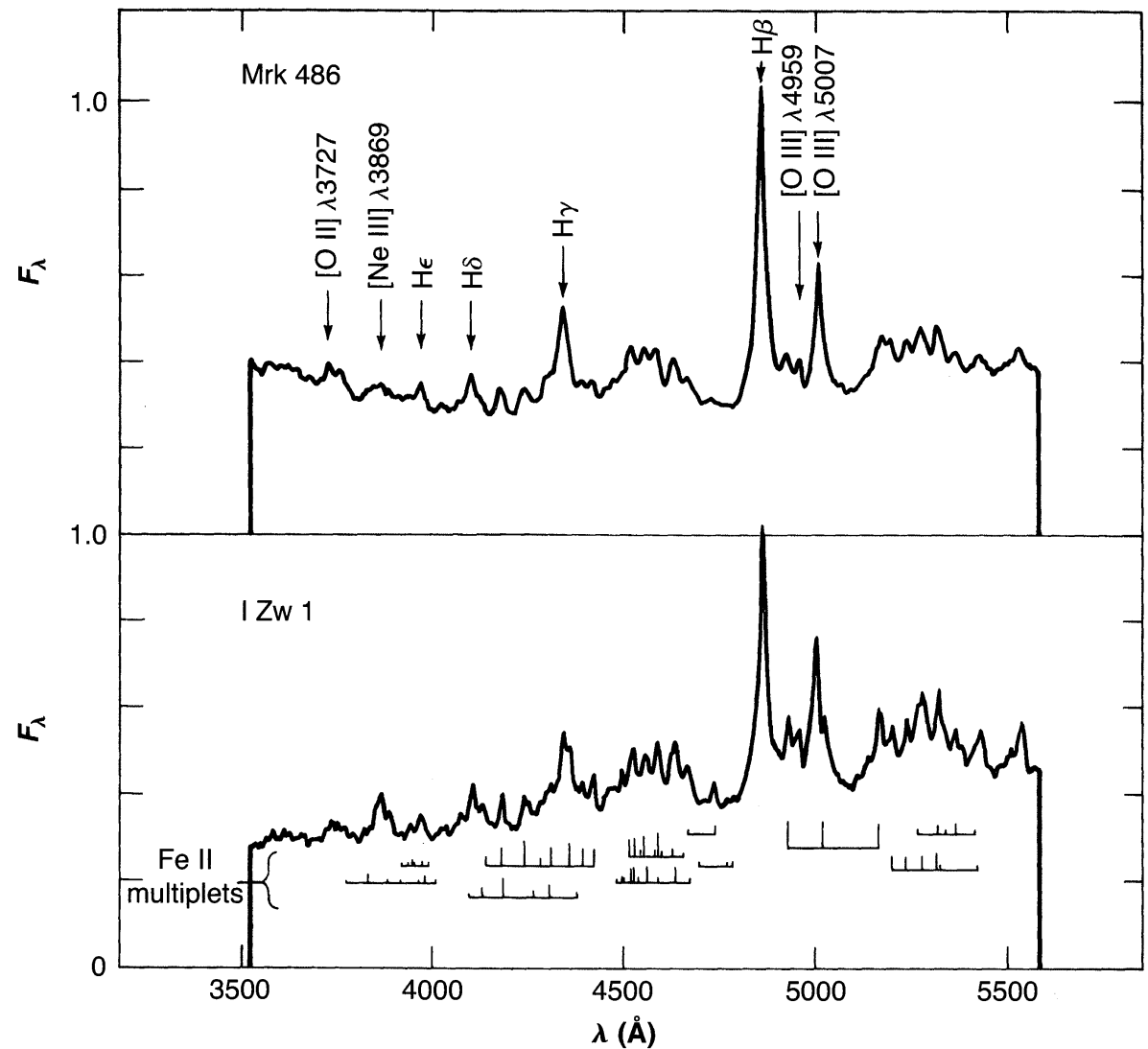


[Figure 14.7]
Spectra of Mrk 486 and I Zw 1, (two Seyfert 1 galaxies) with successively narrower Fe II and H I emission lines.

- Several broad blends of Fe II emission are also seen in UV spectra of AGNs, as shown in Figure 14.1.

In the figure, the broad feature roughly 500 Å shortward of Mg II $\lambda 2798$ is attributed to Fe II.

- The combination of large intrinsic line widths of the BLR, and the rich spectrum produced by Fe II, make it difficult to isolate and study individual Fe II lines.

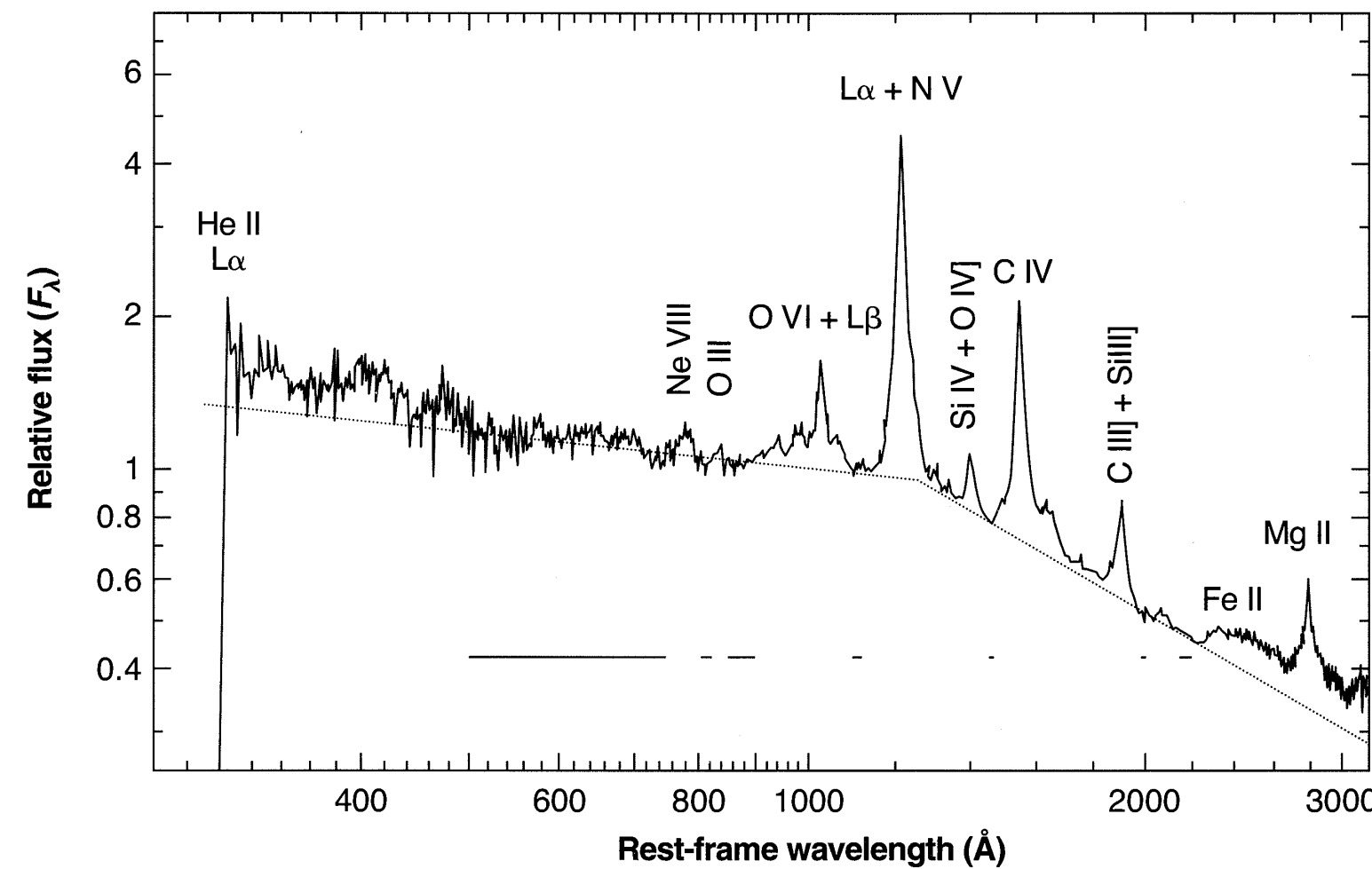
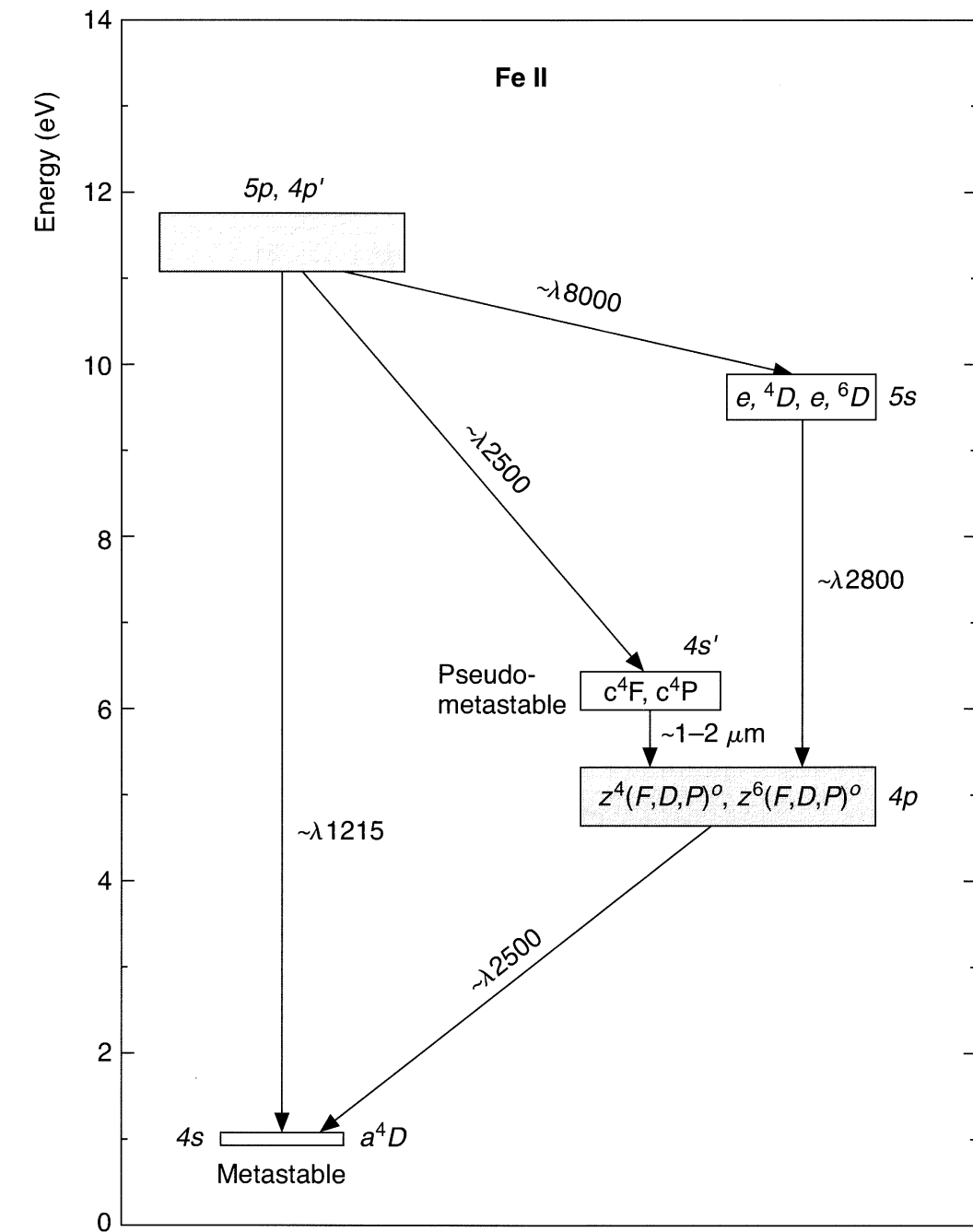
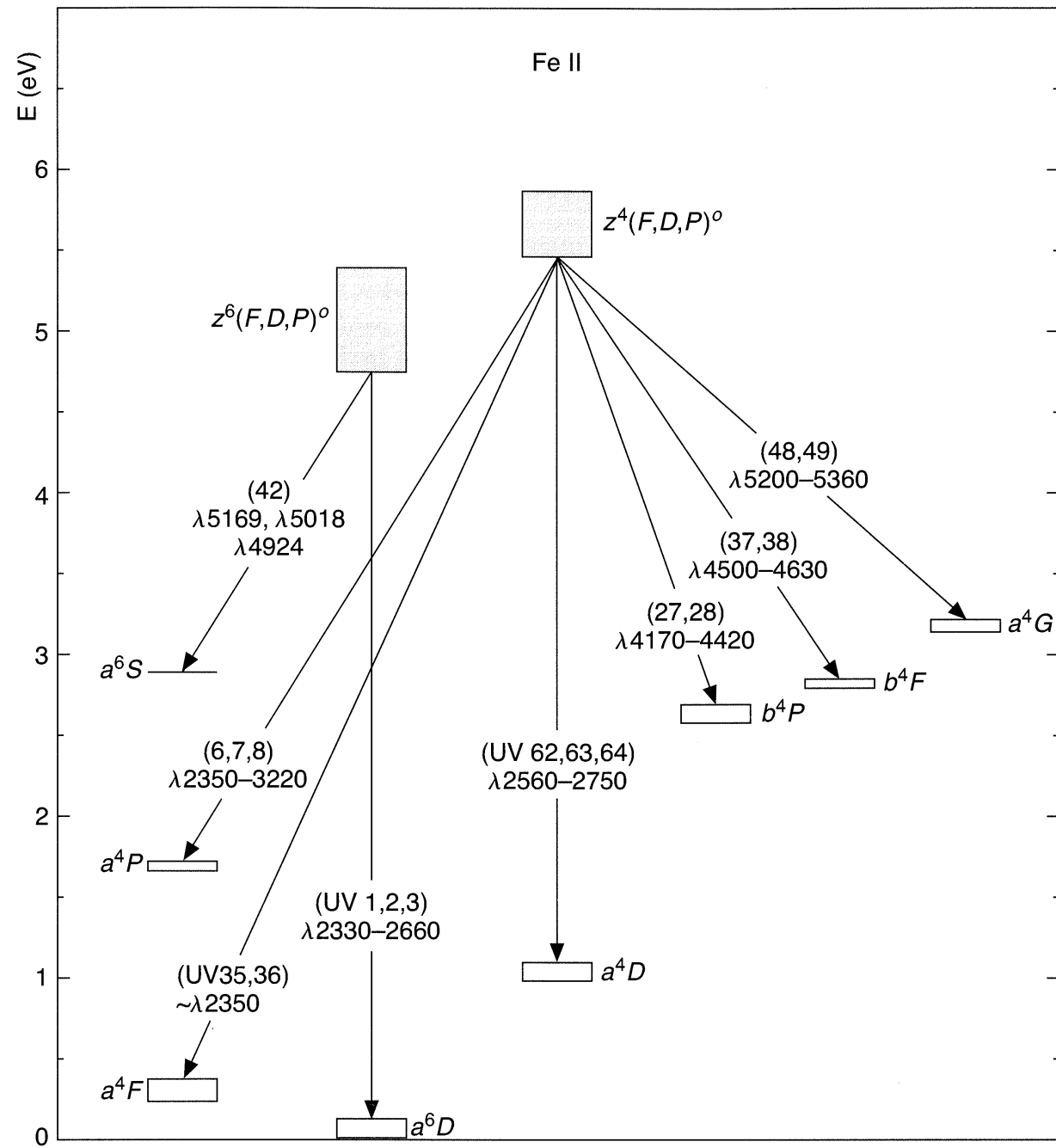


[Figure 14.1] The mean continuum from a sample of intermediate-redshift quasars.

- [Fe II] lines
 - Ground configuration: $1s^2 2s^2 2p^6 3s^2 3p^6 3d^6 4s$
 - The ionization potential of Fe^0 is 7.9 eV and the ionization potential of Fe^+ is 16.2 eV, between those of N^0 and Ne^0 .
 - These lines thus arise in the large, partly ionized transition region of the BLR model (Figure 14.5).
 - The strong optical lines of Fe II come from the energy levels of the terms z^6D^o , z^6F^o , z^6P^o , z^4D^o , z^4F^o , and z^4P^o between 4.8 and 5.6 eV above the ground a^6D term.
 - All the upper levels of the observed optical Fe II lines are connected with the ground a^6D term or the metastable a^4F and a^4D term by strong permitted lines in the UV ($\lambda\lambda 2300 - 2800$).

Therefore, the observed optical Fe II lines are similar to the Balmer lines of H I, while the UV resonance lines of Fe II are similar to the Lyman lines.

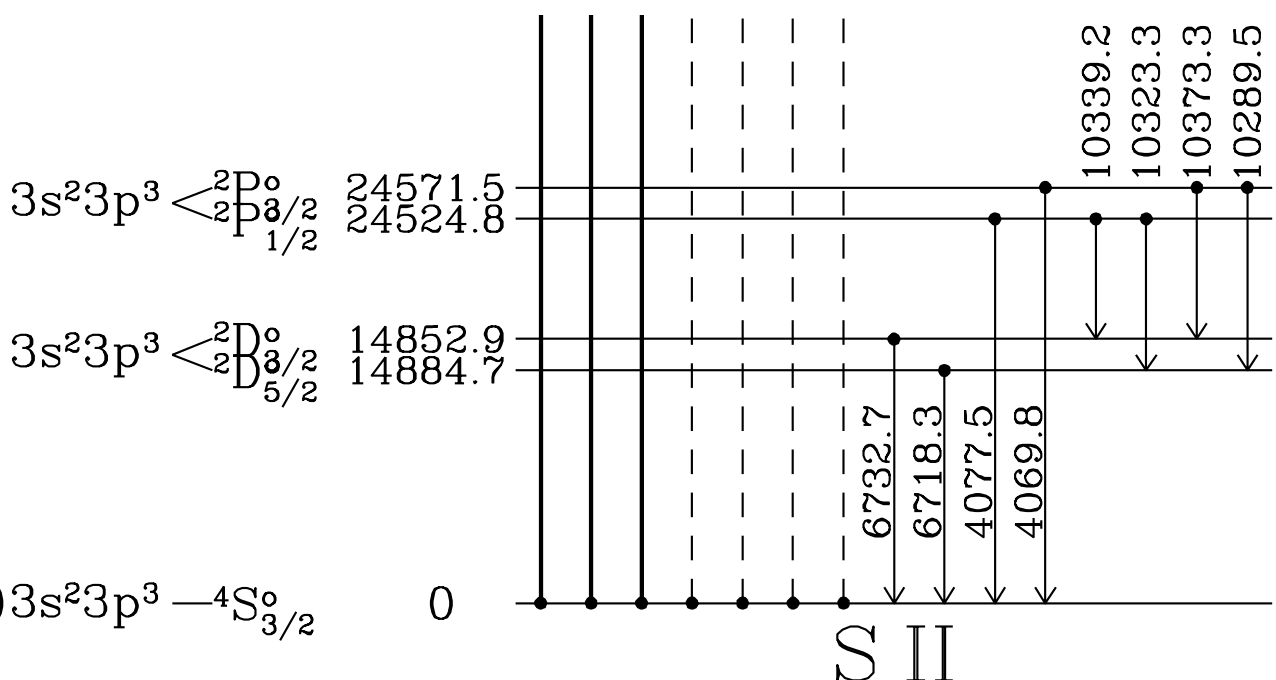
- [Scattering and Fluorescence] The optical depths of the Fe II resonance lines are large, so any photons originally emitted in them are converted by multiple scattering to the longer wavelength optical lines, with more highly excited upper levels.
- The observed Fe II emission is produced by a combination of collisional and resonance-fluorescence processes.
 - ▶ Collisional excitation can populate levels as high as a few eV above ground. But, the strongest Fe II features lie 5-10 eV above ground. Such high excitation would require temperatures above 50,000 K.
 - ▶ Resonance fluorescence, in which a continuum photon is absorbed by a line, can populate very high levels.
 - ▶ The H I Ly α line can populate certain very highly excited levels.
 - ▶ A continuum of collisional excitation and resonance fluorescence by both the continuum and Ly α seems to give the overall best fit to the observed spectrum.
 - ▶ This line formation is an extremely complex one, because Fe II has so many energy levels, and there are so many collisional and radiative transitions that connect them.
 - ▶ Also, the collision strengths and the transition probabilities are not accurately known.



-
- The Fe II permitted emission lines are not observed in PNe and H II regions, although they are seen in T Tauri stars.
 - In T tauri stars, Fe has condensed into solids, while grains have been destroyed by shocks, so that Fe is present in the gas phase.
 - Strengths in Fe II
 - Fe II emission tends to be brighter in radio-quiet AGNs. (Mrk 376, Mrk 486, I Zw 1: three strongest Fe II source)
 - However, a broad range of intensities are observed. The cause of this dispersion is not clear.
 - Goal of investigations of the BLR
 - is to measure the composition of gas so near the center of a galaxy.
 - The large intrinsic line widths make it difficult to measure faint temperature sensitive lines or resolve close density-sensitive doublets.
 - The main results of photoionization models is that the composition of the gas is broadly consistent with solar heavy-element abundances, or perhaps a bit higher, in even the highest redshift AGNs observed so far.

14.6 Dust in AGNs

- Dust is present in AGNs.
 - The emitted light from the NLRs and BLRs must pass through the interstellar media of both the host and our galaxies. In addition, dust may exist within the emitting gas itself.
- Extinction in NLRs
 - The extinction due to dust can be seen in the Balmer decrements of observed NLRs.
 - Most of this extinction appears to arise in foreground material, since large extinctions cannot occur within the H⁺ zone.
 - In a few objects, the [S II] ratios $I(^4S - ^2P)/I(^2D - ^2P)$ (optical-to-NIR ratio) has been measured, and it was found that similar extinctions to the values derived from the H I Balmer decrement.
 - It is nearly always turns out that the intrinsic H α /H β ratio is larger than the recombination value 2.85.
 - This can be understood to result from the contribution of collisional excitation of H α in the partly ionized transition region.
 - However, the ratios of the higher ($1s^2 2s^2 2p^6$) $3s^2 3p^3 \rightarrow 4S_{3/2}^o$ Balmer lines to H β is the same as in the Case B recombination spectrum.



[Draine's book]

-
- Extinction in the BLRs
 - It is more difficult to measure the reddening to the BLR.
 - The H I Balmer-line ratios are modified by optical-depth and collisional effects.
 - ▶ In a plot of $H\alpha/H\beta$ versus $H\beta/H\gamma$, the Seyfert 1 and BLRG nuclei do not cluster tightly around a reddening line, with slope determined by the standard interstellar extinction curve, but with a relatively large scatter about it.
 - The best approach is to use the He II spectrum to estimate the reddening of the BLR spectrum.
 - ▶ The He II Ly α line ($4 \times 10.2 \text{ eV} = 304\text{\AA}$) is absorbed by hydrogen atoms before undergoing many scatterings, so the substantial populations in excited states do not accumulate.
 - ▶ As a result, collisional and radiative-transfer effects do not occur, and the He II $\lambda 1640/\lambda 4686$ (corresponding to $H\alpha/P\alpha\alpha$, $6563\text{\AA}/1.875\mu\text{m}$) ratio should be close to its Case B value.
 - ▶ Reddening estimated in this way has tended to be modest, not as large as seen in Cyg A.
 - Dust is unlikely to exist within the BLR.
 - ▶ First, strong lines of Al, Ca, Si, and Fe are seen in the BLR spectrum. These elements are strongly depleted from the gas if grains are present.
 - ▶ Second, the line-continuum reverberation time scale place the gas so close to the continuum source than solid particles would be heated above their sublimation temperatures.
 - ▶ The dust particles may exist within well shielded parts of the BLR, but they must be destroyed when exposed to the full radiation field of the AGN.

-
- Dust in NLR gas
 - The refractory (내열성) elements mentioned above are missing from the gas phase, suggesting that solids have condensed.
 - The NLR is sufficiently far from the AGN so that the radiation field does not heat the grains to their sublimation temperature.
 - Thermal IR emission, attributed to hot grains, is detected from the NLR.
 - Dust effects
 - Dust can absorb both line and continuum photons.
 - A very important effect of dust is the destruction of Ly α line photons, and other resonance-line photons such as C IV $\lambda 1549$.
 - **The great lengthening of the paths of these photons by resonance scattering makes their absorption by dust much more probable than for neighboring continuum photons.** (This effect has been observed for C IV $\lambda 1549$ in PNe.)
 - Dust absorption of the incident LyC radiation is also important.
 - Dust reemission - IR
 - Radiation absorbed by dust is reemitted in the IR. AGNs are strong IR sources.
 - IR measurements of a very large number of galaxies to wavelengths as long as $100 \mu\text{m}$ clearly show excess heated dust in AGNs. The IR continuum peaks at $\lambda \approx 1\mu\text{m}$, corresponding to dust temperature $\sim 10^3 \text{ K}$, roughly the sublimation temperature for many solids.
 - Dust is present with a range of distances from the nucleus and with a corresponding range of temperature, up to the point where dust particles are destroyed by sublimation.

- Dust reddening corrections
 - It is unlikely that the same extinction correction should be applied to the observed continuum as to the emission lines.
 - Dust is concentrated in or near the same clouds as the gas, and the gas clouds fill only a small fraction of the volume and have a covering factor less than one.
 - Then, the (non-ionizing) continuum may be much less subject to extinction than the radiation from the emission-line clouds.
 - On the other hand, the ionizing continuum incident on the clouds may be more affected by extinction than the non-ionizing continuum.

14.7 Internal Velocity Field

- The characteristic features of the AGN spectra
 - the wide range of ionization covered by their emission lines
 - very broad lines
 - The broadening clearly results from the velocity field in the ionized gas within the AGNs.
 - Therefore, understanding this velocity field and how it arises are crucial for understanding the nature of AGNs.
- Line widths
 - FWHM $\sim 500 \text{ km s}^{-1}$ in NLRs of Seyfert 2 galaxies, noticeably wider than those in the nuclei of starburst or H II galaxies, or absorption lines of the integrated stellar spectra of normal galaxies.
 - The line widths in different Seyfert 2 galaxies range from $\sim 250 \text{ km s}^{-1}$ to $\sim 1200 \text{ km s}^{-1}$. NGC 1068 (often called a “typical” Seyfert 2) has an extreme FWHM = $1,200 \text{ km s}^{-1}$.
- Line profiles
 - The line profiles can be approximately fitted by a Gaussian, but have more extensive wings.
 - They are often asymmetric, with the wing almost always extending further to the blue (shorter wavelengths) than to the red.
 - Different galaxies differ from one another in degree of asymmetry, and in the FWHMs of the various lines.

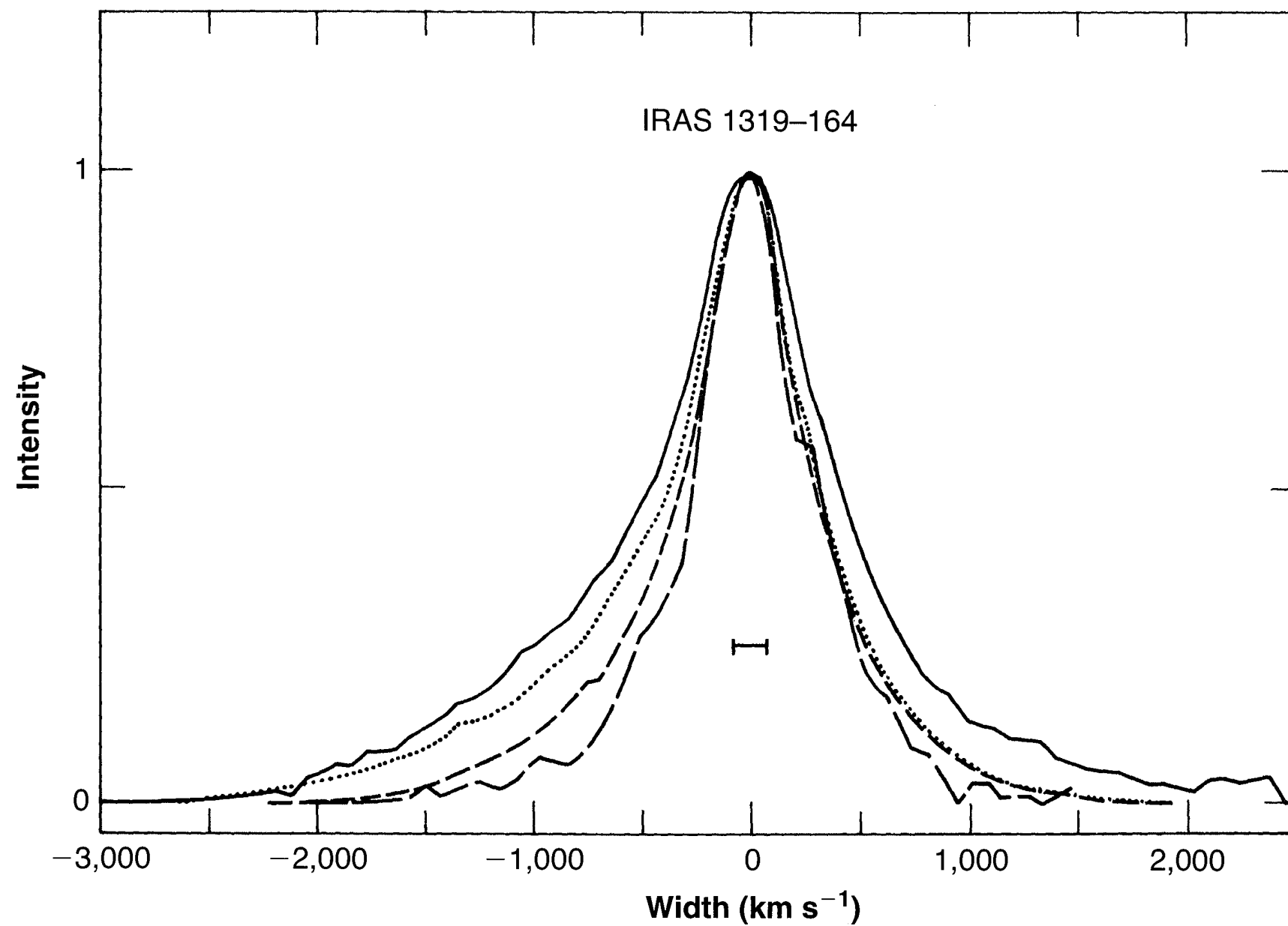


[Figure 14.9]

Line profiles of several lines in IRAS 1319-164, normalized to the same peak intensity.

Solid line - [O I] $\lambda 6300$, Dotted - H α , Short dashed - [N II] $\lambda 6583$,

Long dashed - [S II] $\lambda\lambda 6716, 6731$.

The average instrumental profile FWHM is indicated at zero velocity.

- Correlation between FWHM and Critical density or Ionization Potential
 - The lines with higher critical densities tend to have larger FWHMs.

$[\text{O III}] \lambda 4363$ with $n_c(^1S) = 3 \times 10^7 \text{ cm}^{-3}$ is broader than $[\text{O III}] \lambda 5007$ with $n_c(^1D) = 7 \times 10^5 \text{ cm}^{-3}$ in 70% of Seyfert 2s.

$[\text{O I}] \lambda 6300$ with $n_c(^1D) = 2 \times 10^6 \text{ cm}^{-3}$ is broader than $[\text{S II}] \lambda\lambda 6716, 6731$ with $n_c(^2D) = 2 \times 10^3 \text{ cm}^{-3}$ in 66% of Seyfert 2s.

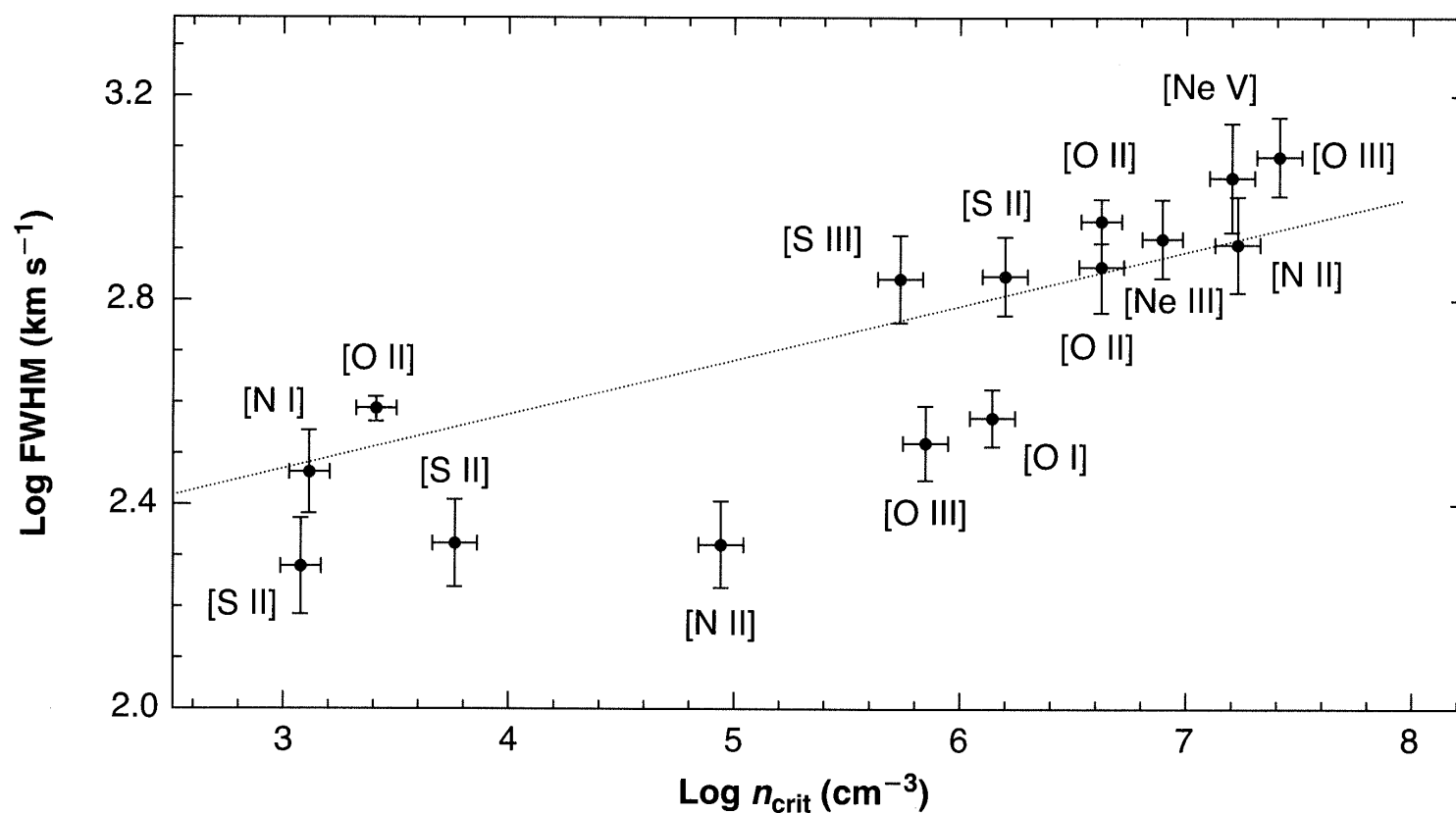


[Figure 14.10(a)]
 The FWHM for various optical and UV emission lines plotted against critical density in LINER M 81. The dotted line gives a least-squares fit to the data.

- The narrow-line profiles in Seyfert 1 and 1.5 are quite similar to those in Seyfert 2s, covering the essentially the same range of widths and exhibiting very similar asymmetries.
- In Seyfert 1 and 1.5 nuclei, there are more tendencies for FWHMs to be correlated with ionization potential.

Ions with higher ionization potential have larger FWHMs.

- However, none of these tendencies is universal. In some members of Seyfert 1 and 2 galaxies, there is little correlation of FWHM with either critical density or ionization potential, or the range in FWHM is small.

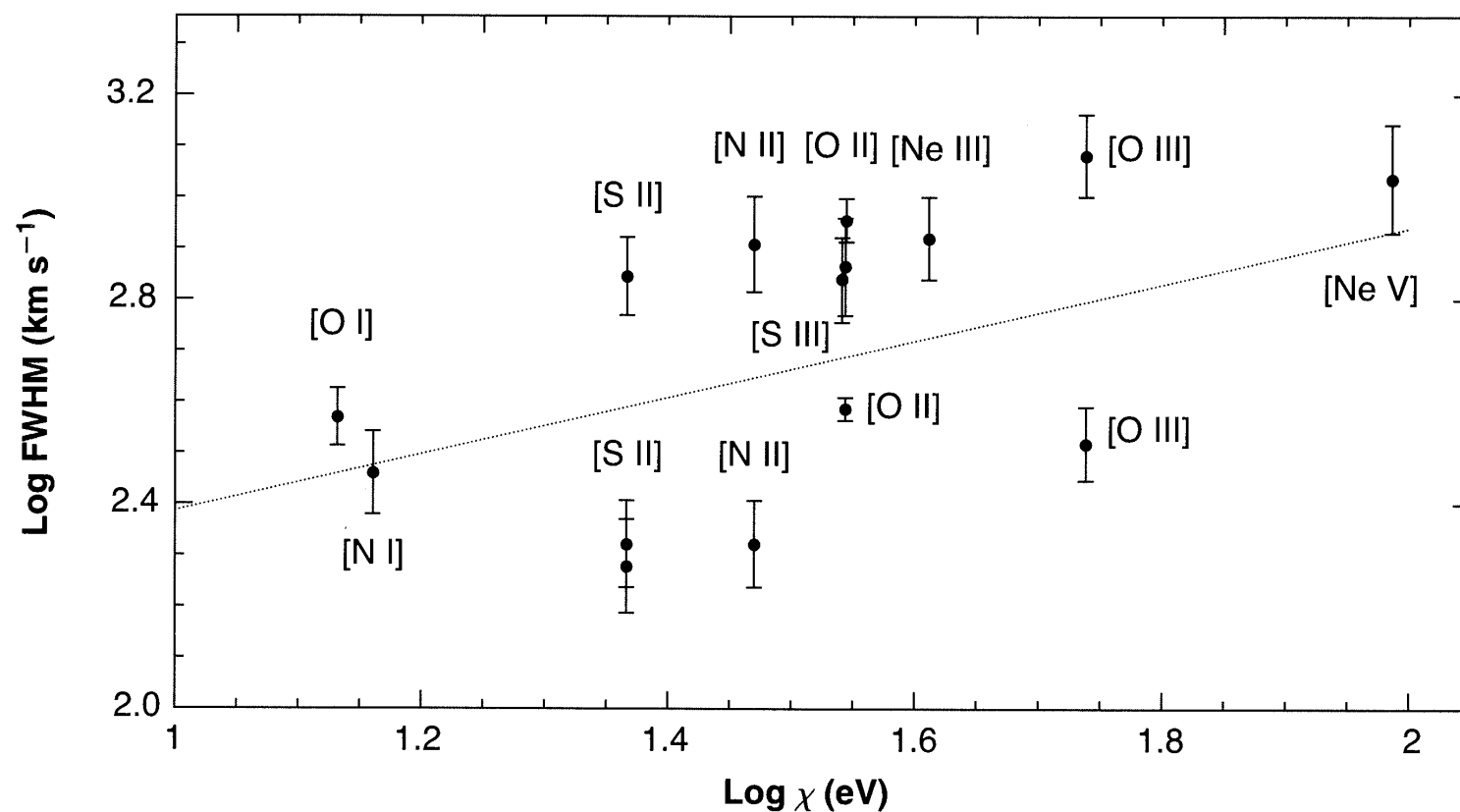


[Figure 14.10(b)]
The FWHM for various optical and UV emission lines plotted against ionization potential in LINER M 81. The dotted line gives a least-squares fit to the data.

- Implications of the correlations
 - There is a range of electron density as well as a range of ionization within the NLR of a given AGN.
 - The highest ionization occurs closest to the central source; the correlation of line width with ionization potential shows that the highest internal velocities also occur there.
 - The region or regions with density near the critical density of any energy level is most effective in the emission of the line (or lines) arising in that level. The correlation with line width indicates that these regions also be nearest the central source.
- Asymmetric profiles, with wings extending to the blue
 - Outflow case
 - ▶ This may result from extinction by dust if the ionized gas is flowing outward more or less rapidly, or more or less perpendicularly to the central plane of the AGN.
 - ▶ **If the dust is mixed with the ionized gas**, line photons emitted on the more distant side of the structure pass through dust on their way to us, and suffer more extinction.
 - ▶ If the farther side is moving away from the central source, fewer photons are observed from the red side of the profile than from the blue side.
 - ▶ Thus, a partially outward, with extinction, seems the best working hypothesis suggested by the observed form of the profiles.
 - Infall case
 - ▶ On the other hand, **if the dust is assumed to be concentrated on the least ionized side of the cloud**, furthest from the central source, then the ionized part of the clouds on the near side of the structure suffer the most extinction. Then, the same line profiles indicate infall.

-
- Dependence of line FWHMs on the density profile

[Density] If the hydrogen density decreases radially outward as a power law in distance,

$$n_{\text{H}} \propto r^{-m}$$

then, since the flux of ionizing photons decreases as r^{-2} , the ionization parameter at the face of the cloud is

$$U = \frac{Q(\text{H}^0)}{4\pi r^2 c n_{\text{H}}} \propto r^{m-2}$$

[Velocity] The velocity field is assumed to be large near the central source.

- If $m = 2$, U and hence the degree of ionization at the front surface of all the clouds is independent of distance.
 - ▶ If each cloud is optically thick, the degree of ionization decreases to zero with increasing optical depth within it, and all clouds have the same ionization and thermal structure.
 - ▶ Hence, even though the velocities of the clouds would depend on distance, the line profiles would not depend on ionization potential at all. On the other hand, the density variation would lead to collisional deexcitation in clouds and thus to a dependence of line profile on critical density.
 - ▶ This observed in many objects, in the sense that higher critical densities are correlated with larger FWHMs.

- If $m > 2$, U would increase outward.
 - ▶ High stage of ionization like Ne^{+4} and Fe^{+6} would not exist in clouds close to the central source.
 - ▶ The FWHM would decrease with increasing ionization potential.
 - ▶ This situation has not been observed in any AGN; therefore, $m > 2$ does not occur in nature.
- If $m < 2$, U decreases outward
 - ▶ High stage of ionization can occur only in clouds close to the central source.
 - ▶ The FWHM would therefore increase with increasing ionization potential.
 - ▶ This is observed in many Seyfert galaxy nuclei.
- If $m = 0$,
 - ▶ There would be no dependence on distance, and hence no correlation of FWHM with critical density.
- Observationally, FWHMs correlate with both n_c and ionization potential.
 - ▶ Therefore, $0 < m < 2$, say $m \approx 1$.
 - ▶ More Seyfert 1s have FWHMs correlated with ionization potential - they tend to have $m \approx 0$.
 - ▶ More Seyfert 2s tend to have FWHM correlated with critical density - they have $m \approx 2$.

- What drives the flow out?
 - One possibility is radiation pressure. The main effect would be from continuum absorption by embedded dust. However, if it is effective in accelerating the clouds, it appears that it will also disrupt them.
 - The NLR is likely to be illuminated face of a number of massive molecular clouds arranged as a torus around the central black hole.

The molecular clouds provide a large reservoir of cold material which can replenish the gas driven off as a wind.
 - Whatever the mechanism, the observational data indicates that the velocity has an outward component which decreases outward.
- Broad lines
 - There is not common asymmetry in the broad lines, as there is in the narrow ones.

In some Seyfert 1 nuclei, the broad lines are symmetric. In others, they are asymmetric with a stronger blue wing, and in others, they are asymmetric with a stronger red wing.

Hence, the physical explanation of the velocity field in the BLR cannot be symmetric radial flow alone, with extinction.
 - A likely velocity field for the BLR is rotation under the gravitational field of the central black hole. This gives a symmetric line profile whether there is extinction or not.

Asymmetric profiles, some to the red and some to the blue must be modeled on this picture by deviations from symmetry in the object, either in the distribution of extinction or in the distribution of the gas in the BLR.

The rotational picture, possibly with outflow also, is very attractive.

- The lag between a continuum variation and the response of the emission lines varies with ionization potential.
 - More highly ionized species have shorter lags and must lie closer to the central object.

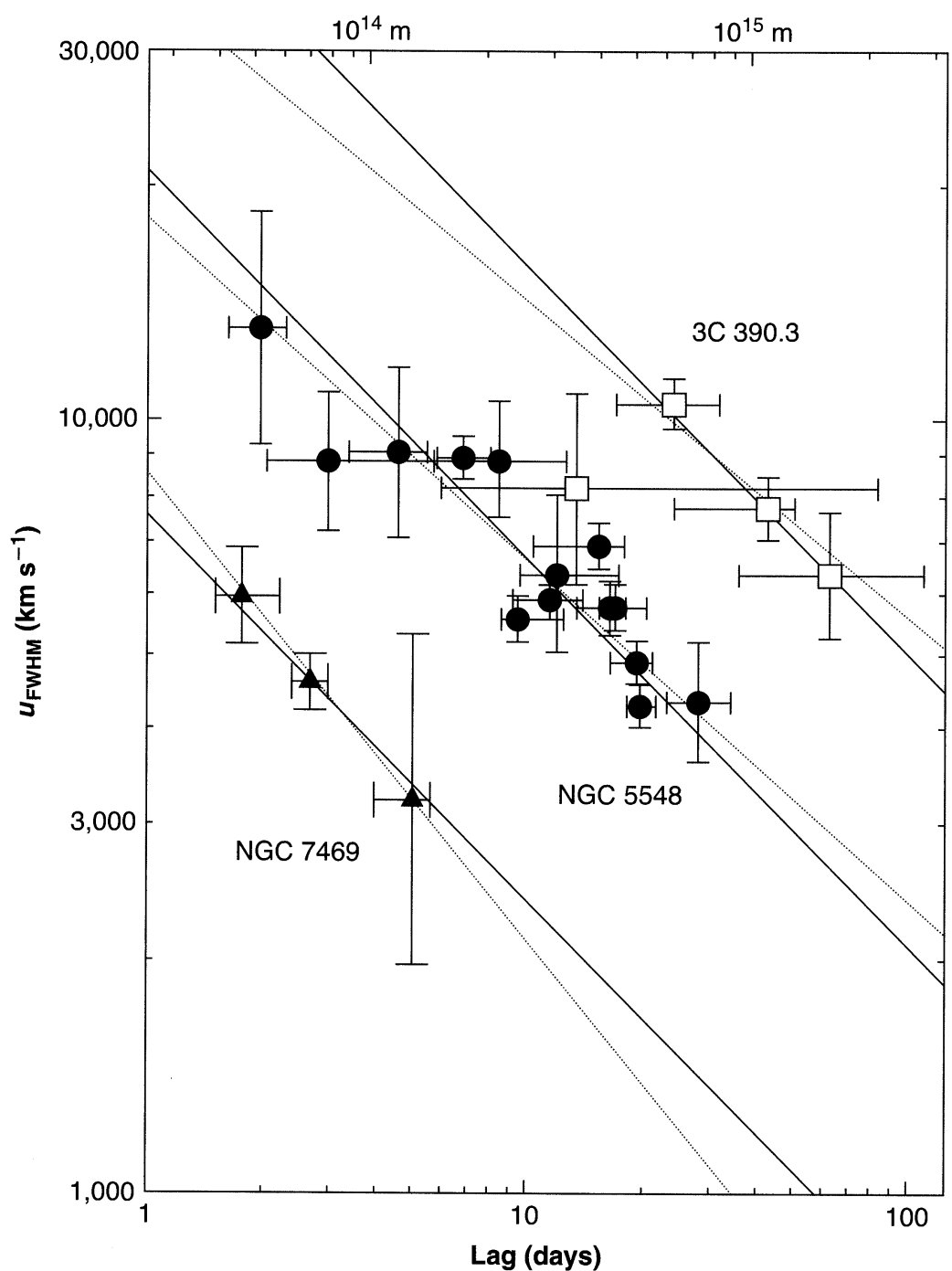


Figure 14.11

The line-width continuum-lag correlation for two Seyfert galaxies and the broad-lined radio galaxy 3C 390.3. The lower x axis gives the measured lag between continuum and line variations, an indication of the distance where the line forms. The FWHM for each line is given on the y axis. The slope of the heavier lines is given by Equation (14.15), as described in the text.

14.8 Physical Picture

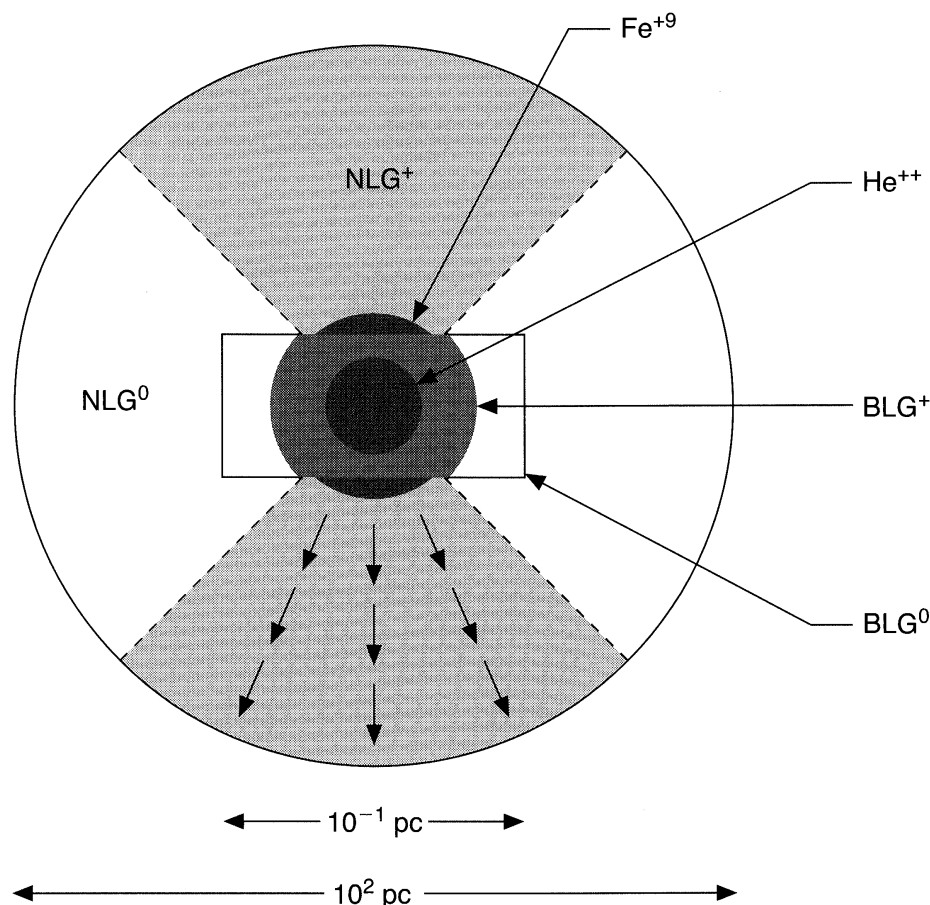


Figure 14.13

Schematic AGN model, showing the central photoionization source as a black-filled circle, broad-line gas (BLG) in a disk ionized near the source and neutral further away, and narrow-line gas in much larger sphere, ionized in the cone in which ionizing photons can penetrate the broad-line gas and escape. Note that the scale is distorted in the interest of legibility.

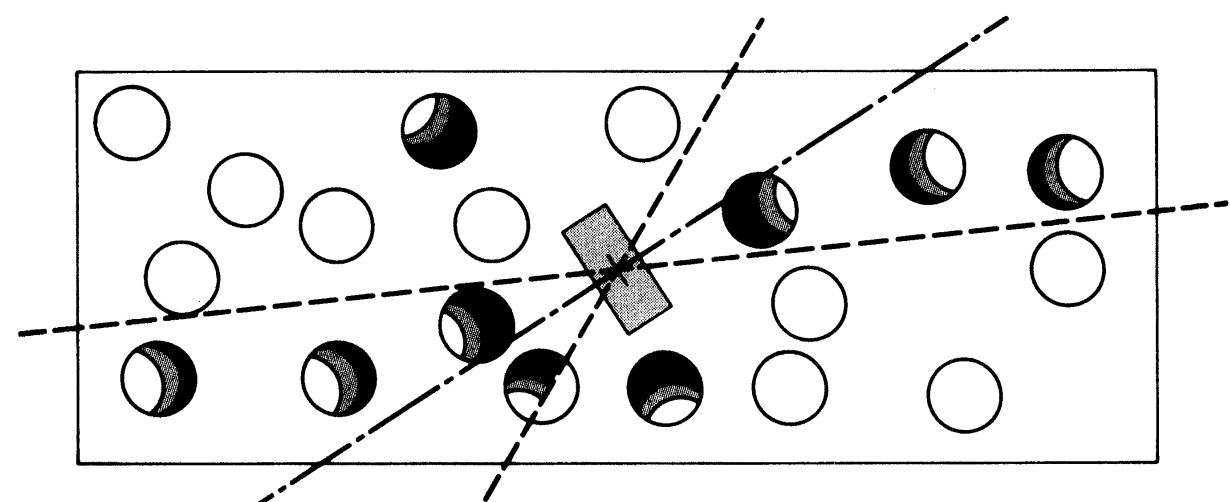


Figure 14.14

Schematic AGN model, showing tipped broad-line disk in larger narrow-line disk, with cloud structure indicated schematically as spheres. The ionizing photons mostly escape through the broad-line disk in the cone around its axis, but a few routes for escape also may exist even near its equators. Highest degree of ionization, indicated by darkest shading, occurs only in clouds nearest the central source (for uniform density clouds).

- **Polarization**

- Measurements of the polarization of the emission lines and the continuum in Seyfert galaxies show that many Seyfert 2s have hidden Seyfert 1 nuclei.
- The polarization is independent of wavelength over the observed range $\lambda\lambda 3500 - 7000$.
 - ▶ Electron scattering has this property.
 - ▶ Interstellar dust particles do not.
 - ▶ However, the electron temperature must be $< 10^6$ K, because otherwise the lines would be thermally broadened by an amount greater than their observed widths.

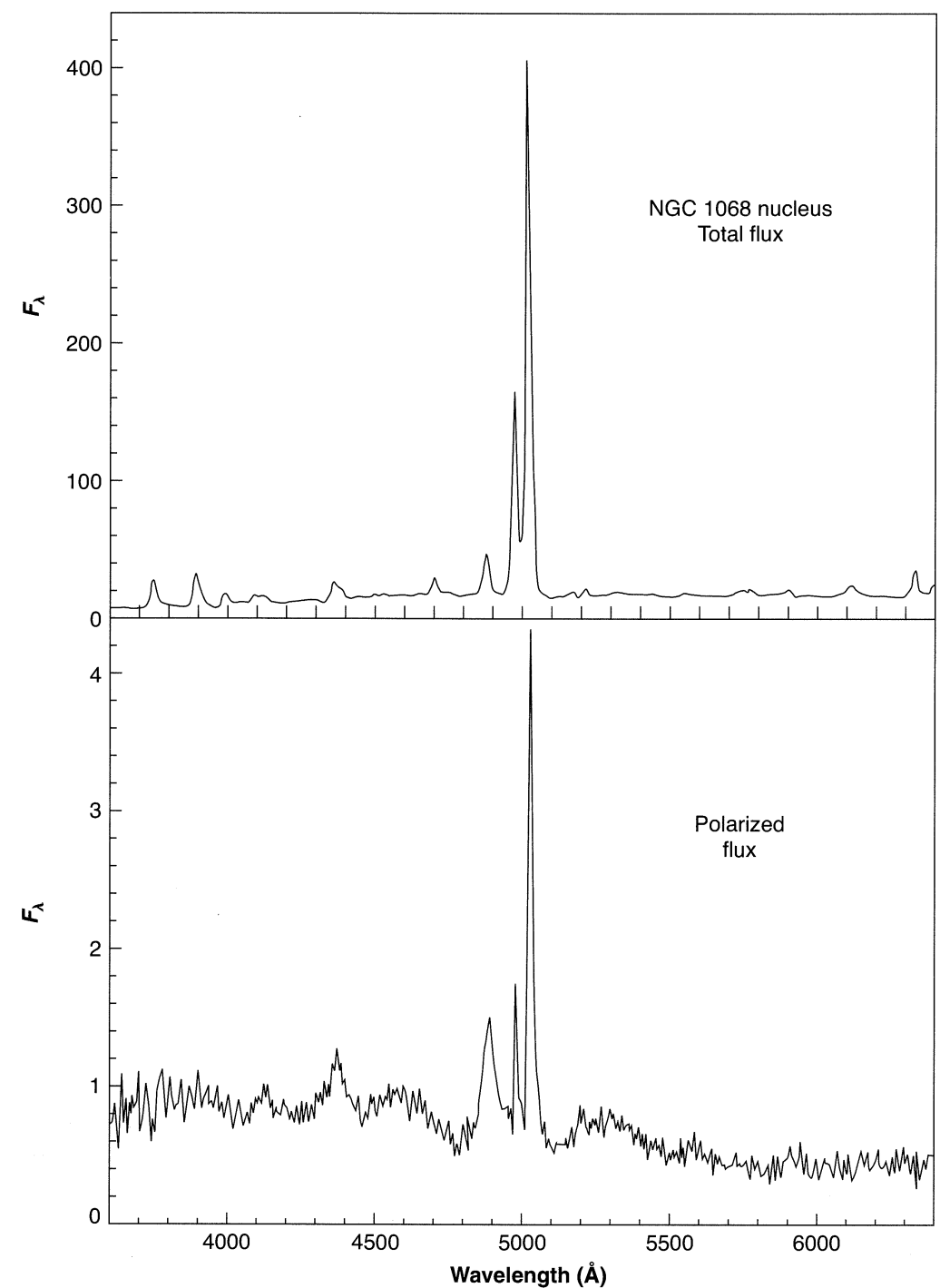


Figure 14.15

The white-light spectrum of the Seyfert 2 galaxy NGC 1068 is shown in the upper panel. The lower panel shows the spectrum observed in plane-polarized light. The hidden BLR is visible in polarized light, which can detect the small amount of reflected light in the system.